Assessment of Battery Lifetime for Power Grid Services

Master Thesis

Guillem Gómez Talero

Aalborg University
Energy Department

Here you can write something about which tools and software you have used for typesetting the document, running simulations and creating figures. If you do not know what to write, either leave this page blank or have a look at the colophon in some of your books.

Energy Department
Aalborg University
http://www.aau.dk

AALBORG UNIVERSITY
STUDENT REPORT

Title:
Assessment of Battery Lifetime for Power Grid Services

Theme:

Scientific Theme

Project Period:

Spring Semester 2025

Participant(s):

Guillem Gómez Talero

Supervisor(s):

Florin Iov
Daniel-Ioan Stroe

Copies: 1

Page Numbers: 63

Date of Completion:
May 27, 2025

Abstract:

There has been a significant increase in renewable energy deployment recently. These sources are variable and can cause grid instability. Integrating Energy Storage Systems (ESS) with photovoltaic (PV) plants helps mitigate these fluctuations and provides grid services following Transmission System Operator (TSO) regulations.
Lithium-based batteries, especially lithium iron phosphate (LFP), are preferred for Hybrid Power Plants (HPPs) due to their efficiency, fast response, long life and environmental benefits. This thesis uses an LFP battery.
Battery lifetime is crucial for project feasibility. This work analyzes degradation from capacity loss while providing primary frequency regulation (Frequency Containment Reserves, FCR), capacity firming with 15-minute schedule steps and both services combined.
A real one-year mission profile is used for frequency, irradiance and temperature. The battery reaches End of Life (EOL) after losing 20% capacity. Under these services, lifetime is about 5 years, varying slightly by service.

Contents

Preface

Aalborg University, May 27, 2025

Guillem Gómez Talero
<gtaler23@student.aau.dk>

Chapter 1

Introduction

1.1 Background and Motivation

Nowadays, there is an increasing adoption of renewable energy systems (RES) as it shown in Figure 1.1 and reported by the IEA (International Energy Agency) [1].
These technologies face several challenges, one of the main ones being their higher variability compared to traditional energy sources. This is due to their dependence on natural resources like sunlight and wind, which are difficult to predict with precision.

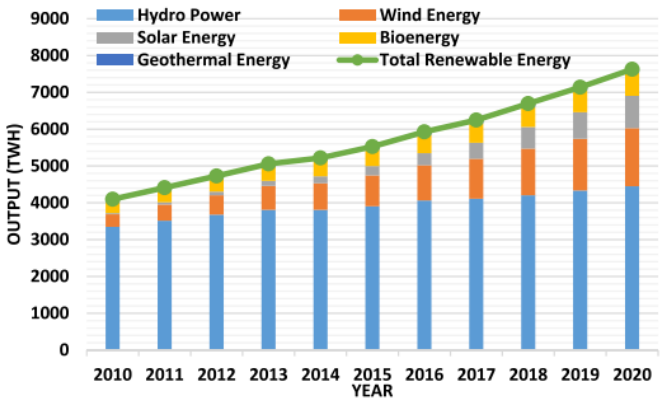

Figure 1.1: Total renewable energy usage (2010–2020)
[1]

For this reason, hybrid power plants have begun to be developed, integrating these renewable energy sources with batteries or other forms of energy storage. The aim is to solve the problem of the variability of these energy sources and to always be able to supply energy without the fluctuations between the generation and demand, maintaining a certain quality defined by the TSO (Transmission System Operator). However, there are

different services depending on whether it is necessary to control the frequency because it is rising or falling, or the power delivered to the grid according to demand. Consequently, these different services will have varying impacts on the battery connected, in this case, to a solar plant. Therefore, battery degradation will be calculated and its lifetime estimated while performing different services. The results may provide valuable insights into how to determine the costs associated with integrating the battery into the PV plant, and how these costs can be amortized over time. For this reason, the primary motivation for analyzing the battery's lifetime is ultimately economic. Even though an economic study will not be developed in this project, understanding the technical aspects of degradation is essential for future cost assessments.

The motivation of this project is to address the challenge of variability in renewable energy generation and its impact on the performance and lifespan of batteries in hybrid systems. Additionally, in electricity markets, bids have shifted from being made on an hourly basis to every 15 minutes[2]. This change could potentially lead to more accurate forecasts, as it is easier to predict what will happen in the next 15 minutes than over the course of an entire hour. As a result, the battery may need to be used less frequently. However, if not managed properly, this approach could actually result in more frequent usage of the battery, since it would be operated several times per hour instead of just once under an hourly bidding scheme.

Therefore, by understanding and measuring battery degradation under different services, the project aims to optimize system performance, enhance energy stability and reliability, and facilitate a sustainable and economically viable transition to renewable energy sources, while ensuring compliance with the quality standards established by the TSO.

This project focuses on analyzing data from a solar plant integrated with an electric battery in Denmark; therefore, it must follow and comply with the regulations of the country's TSO, specifically Energinet. This country is divided into two well-distinguished parts by its electricity market: one market is DK1 and the other is DK2, as shown in Figure 1.2.

Figure 1.2: DK1 and DK2
[3]

It's important to highlight this because each has different interconnections with other countries and varying levels of renewable energy penetration, which affect their energy prices. They also offer different services with varying requirements, as well as differences in ancillary services[4].

In this project, the regulations according to DK1 will be followed, and it will focus on two different services. The first service occurs when there is a difference between the actual power generated and the expected power. In this situation, if less power than expected is generated, the battery must supply the difference to fulfill the previously made bid, thus avoiding penalties and helping to maintain grid balance. This concept is known as capacity firming or grid firming[5].

The second service involves the battery meeting the requirements of Frequency Containment Reserves (FCR), which is an ancillary service. In this case, the battery helps maintain the frequency within a range between 49.8 Hz to 50.2 Hz at all times, the purpose is to achieve faster power balancing.

The project aims to analyze battery degradation in each of these scenarios individually, as well as when the battery performs both functions simultaneously.

1.1.1 Capacity Firming

As previously mentioned, one of the services to be provided is capacity firming. In this project, this service will be implemented by comparing the difference between the actual power obtained every 10 seconds and the power schedule steps every 15 minutes, which will be generated using a moving average of the actual 10-second data.

No forecasting is performed in this project since real data is used. However, in a different scenario, the better the forecast of the solar plant, the less this service would need to be used, because the generated power would match the predicted one, and therefore the bid made would be accurate. Otherwise, the battery would need to be used to adjust the energy injected into the grid so that it matches the submitted bid.

If a bid is made in the market and it is not fulfilled, monetary penalties may be imposed. Therefore, it is a strong incentive to produce an accurate forecast or to be able to provide this service by adjusting the generated energy to match the market offer.

1.1.2 Ancillary services

In any power system, there must always be a balance between generation and electricity demand. Any change in demand or variation in generation will affect the system's balance, causing a frequency deviation. This is why Energinet purchases ancillary services, allowing them to be used at any time to maintain the stability and reliability of the electrical system[6].

There are two ways to supply ancillary services:

- The supplier must be approved as a balance-responsible party for either generation or demand and must also have signed a "Main agreement on the delivery of ancillary services". This option provides access to the delivery of all ancillary services covered by present Tender conditions.
- The supplier must have signed an "Agreement on the delivery of balancing services without energy supplies". This option provides access to the delivery ancillary services with very limited energy supplies, which do not require that the supplier has a contract with a balance responsible party.

The different systems that will provide ancillary services must be approved by Energinet. Additionally, turbines or PV systems without backup can submit their bids in different ancillary services markets, provided that the market participants handling these energy sources in the electricity market are able to produce a forecast of sufficient quality and an accurate baseline calculation.

The following ancillary services to be delivered in DK1 are covered by these tender conditions:

- Primary reserve, FCR
- Secondary reserve, aFRR
- Manual reserves, mFRR
- Properties required to maintain power system stability.

The Frequency Containment Reserves (FCR) is the fastest ancillary service and has the shortest activation time and this ensure the frequency does not deviate too much. The purpose of frequency containment reserves is to immediately add power to the system to restore the frequency, preventing that the frequency becomes either too low or too high. Automatic Frequency Restoration Reserve (aFRR) and Manual Frequency Restoration Reserve (mFRR) are the slower ancillary services with longer activation time and are meant to release frequency containment reserves, making these services ready to handle new frequency deviations and thereby restoring balance in the power system[4].

The FCR is an essential service for maintaining the balance between electricity generation and demand in real-time, ensuring frequency stability not only in the Danish electrical system but also across European grids. In 2017, the FCR Cooperation was established with several TSOs from European countries, where participating TSOs jointly procure FCR capacity through common auctions. Each TSO is responsible for its balancing service providers (BSPs) within its control area, managing contracting, control, and settlement[7]. Denmark, through Energinet, is required to provide approximately ±23 MW of FCR per hour in 2023 as part of the total ±3,000 MW requirement for the Continental European synchronous area. Additionally, Danish market participants can export up to 100 MW, meaning Denmark has the potential to contribute up to 123 MW of FCR per hour. This contribution is part of the cooperation among European transmission system operators (TSOs) to maintain frequency stability in the power grid[6].

On the other hand, Energinet procures primary reserves as a single symmetric product. A daily auction is held for the upcoming operational day. For the purpose of the auction, the 24-hour period is divided into six equally sized blocks of four hours each. Bids must be submitted to the Regelleistung internet platform by 08:00 a.m. on the day before the operational day. Bids must state a quantity and a price for each four-hour block, and the minimum size for bids is 1 MW. Bids must always be stated in MW without decimals, and the price must be stated in EUR/MW to two decimal points[6].

1.1.3 FCR in DK1

In this project, despite the fact that DK1 has several ancillary services, such as aFRR and mFRR, as mentioned previously, we will focus solely on how FCR, which is the primary and fastest frequency control, affects an electric battery when it is activated. The idea of FCR is to maintain grid stability; therefore, the goal is to keep the frequency within a range defined by the grid code. Figure 1.3 graphically illustrates this process.

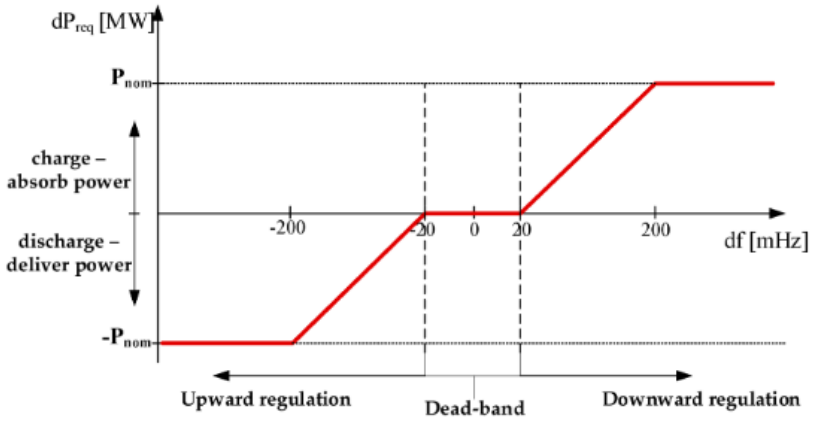

Figure 1.3: Frequency regulation with FCR [8]

The frequency can vary by a maximum of ±200 mHz, meaning it can range between 49.80 Hz and 50.20 Hz, with a permitted deadband of ±20 mHz [6]. As shown in Figure 1.3, when there is a frequency drop, it indicates a higher power demand that is not being supplied. Therefore, power is injected through the battery to balance the system.

On the other hand, when there is a frequency increase, it means that more power is being generated than consumed, requiring additional loads to absorb the excess energy or, in this case, using the battery to store it.

A primary control mechanism like this can be explained by the Equation 1.1 related to classical synchronous generators in conventional power plants, which explain the relation between the frequency and the power through the droop[9].

$$R_{\%} = \frac{\Delta f_{\%}}{\Delta P_{\%}} = \frac{\omega_{nl} - \omega_{fl}}{\omega_0} \cdot 100\% \tag{1.1}$$

In this case, R represents the droop, Δf the frequency variation, and ΔP the power variation. ω_{nl} is the no-load angular velocity, while ω_{fl} corresponds to the full-load angular velocity. The term ω_0 represents the nominal angular velocity.

1.1.4 PV and battery sizing

To design and size both a solar power plant and a battery would be a project in itself. Therefore, general guidelines will be followed to select the type of solar power plant and battery to be used in this project, taking inspiration from existing MW pilot projects worldwide.

In the case of the solar power plant, a type C or type D plant can be used, following Energinets regulations [10], as they require frequency control available from these plants types. In this work, the degradation of the battery will be analyzed when used for FCR, in addition to capacity firming. The difference between these two types is the installed capacity as shown in Table 1.1.

Type	Power
C	1 MW – 25 MW
D	> 25 MW

Table 1.1: Solar Power Plants Types

For the battery case, the same applies: it will be classified as either type B or C, which have the corresponding power values shown in Table 1.2[10]. The specific battery type to be used will be decided later.

Type	Power
B	125 kW – 3 MW
C	3 MW – 25 MW

Table 1.2: Battery Types

In fact, there are currently several hybrid power plants, and more are planned in the country. One of the companies actively developing these projects is Eurowind, which operates hybrid parks integrating PV, wind, batteries, and power-to-X technologies [11]. When sizing the battery, it is crucial to consider the power that will be drawn from it, as well as the charge and discharge cycles. To achieve this, an accurate forecast of the solar plant's irradiance must be performed beforehand, since the amount of power the battery needs to provide will depend on this factor. The power exchanged by these hybrid systems with the grid at any given time instant can be worked out as:

$$P_{\text{grid}}(t) = P_{\text{PV}}(t) + P_{\text{ES}}(t) \tag{1.2}$$

Where P_{grid} is the power supplied at all times by P_{PV} through the solar panels, and P_{ES} is the power provided by the battery to complement the panels. Ideally, if the forecast is

well modeled, most of the power will be supplied by the panels without the need to use the battery, or only minimally, thereby reducing battery degradation [12]. In this project, no forecast will be created. The usage of the battery will be analyzed performing the different services. As mentioned in subsection 1.1.1, it is important to comply with the submitted bid by delivering the committed energy, as failing to do so will result in a financial penalty.

1.2 State of Art on Mission Profiles and Battery Lifetime

This project aims to analyze the impact of the mission profile on battery degradation when providing different services.

Within the literature on solar power plants integrated with battery storage systems, there are several aspects that require further investigation and improvement. One key area is solar forecasting, which has been addressed in various studies [13, 14]. These studies explore different forecasting methods, their accuracy, and how machine learning can be leveraged to generate predictions based on historical data. It is noted that most of these studies produce forecasts on an hourly or daily basis. However, more granular forecasts or real-time data at 15-minute intervals would be more appropriate, given that recent energy market bidding processes are conducted at such time resolutions. Moreover, some studies neglect crucial parameters such as temperature, solar irradiance, or cloud cover.

To address this gap, the present study provides high-resolution real-world data—solar irradiance and temperature measurements recorded every 10 seconds over an entire year. This level of detail enhances the accuracy and reliability of solar plant modeling.

Several challenges and areas for improvement motivate the development of this project. One of the primary objectives is to assess battery degradation while delivering the capacity firming service, using real data collected over a full year. Additionally, this work aims to examine the combined provision of Frequency Containment Reserve (FCR) and capacity firming services, evaluating their joint impact on battery degradation.

Regarding FCR, previous studies have analyzed battery degradation using real operating data over annual cycles. One study investigates different strategies for delivering FCR and their corresponding effects on battery aging [15], while another delves into the influence of temperature and State of Charge (SoC) on battery degradation during FCR operation [16]. In the present work, FCR analysis will also be performed using real data sampled every 4 seconds over a one-year period.

Furthermore, a recent study explores the optimization of a Battery Energy Storage System (BESS) by combining peak shaving and FCR services [17]. However, it does not evaluate battery degradation in terms of capacity loss, nor does it examine the individual

contributions of each service to the aging process and the overall lifetime of the battery.

Therefore, this project aims to provide valuable insights into battery degradation under different operational scenarios, whether services are delivered independently or concurrently.

1.3 Project Objective

The main goal of this project is to assess and analyze battery degradation in order to estimate battery lifetime. This overall objective is divided into the following three specific objectives:

- Propose a framework for generating realistic operational profiles corresponding to different grid services.
- Assess the impact of two individual services on battery lifetime.
- Evaluate the combined impact of both services on battery lifetime.

1.4 Methodology

This study analyzes battery degradation connected with a solar power plant located in a specific area of Jutland, Denmark, operating under both Capacity Firming and Frequency Containment Reserves (FCR) services.

On one hand, real irradiance data, recorded every 10 seconds throughout an entire year, along with temperature data, will be used to compute the output power of the PV plant. A moving average will be applied to this power signal to generate scheduled power setpoints every 15 minutes, corresponding to the bids made in the electricity markets. The difference between these scheduled setpoints and the actual 10-second data will determine the power demand the battery must meet to provide the Capacity Firming service.

On the other hand, frequency data recorded every 4 seconds will be used to assess battery degradation under FCR operation.

Through simulations, three operational scenarios will be evaluated: one where the battery mitigates solar generation deviations (Capacity Firming), another where it provides frequency regulation (FCR), and a third where it delivers both services simultaneously.

After simulating all scenarios, battery degradation will be evaluated using the modeling equations presented in [16]. Degradation will be divided into two components: one occurring when the battery is in idling mode (i.e., zero power), and another during cycling.

Once both contributions are obtained, they will be summed to estimate the annual degradation. A linear extrapolation will then be performed to determine the battery's expected lifetime, defined as the point when it reaches 80% of its nominal capacity (End of Life).

Once the degradation results are obtained, they will be analyzed and the findings will be summarized in the conclusions.

1.5 Scope and Limitations

1.5.1 Scope

The project will focus on how frequency control, capacity firming, and the combination of both affect the battery degradation and thus lifetime. The design and sizing of the battery or the solar plant will not be addressed, as these topics would constitute separate projects on their own. The same applies to the inverter in the PV plant and the battery; it will not be considered in this project. No forecast will be made as real irradiance data is available for a year, and it has been obtained every 10 seconds, which will provide much more accurate data. The capacity firming will be done with this real data and the moving average of this data every 15 minutes to align with the bids made in the electricity markets. The motivation for this study is primarily economic, as mentioned in section 1.1. By estimating the battery's lifetime, it becomes possible to design systems accordingly or to evaluate how the investment could be amortized over time.

1.5.2 Limitations

In this project, several limitations arise due to the different models used:

- The PV plant model used to obtain the output power is not the most accurate. Although it uses real measured irradiance and temperature as inputs, more advanced models exist with more complex equations or additional factors that could yield more accurate estimations of the generated power.
- The moving average model creates schedule steps every 15 minutes by averaging the real measured data from the previous 15 minutes (sampled every 10 seconds). More accurate scheduling could be achieved using other techniques or artificial intelligence methods.
- The battery model used in this study only corresponds to LFP-Lithium Iron Phosphate($LiFePO_4$) chemistry. Therefore, the results of this study are not applicable to other battery chemistries.
- It is important to note that this project does not include any economic analysis.

1.6 Content of report

This report begins by introducing the topic of hybrid power plants with integrated battery storage, explaining their necessity and the different services they provide. Following this, the location of the solar plant will be determined. Once these foundational aspects are established, different operating scenarios will be analyzed to assess how the battery interacts with the solar plant. Finally, the study will focus on evaluating battery degradation under these scenarios, providing insights into its long-term performance and potential optimization strategies.

Chapter 2

System Characterization

2.1 System Structure

As mentioned in the previous chapter, this work will focus on analyzing degradation of the battery with different services. To achieve this, the system has been represented in a line diagram to illustrate its various components, as shown in Figure 2.1.

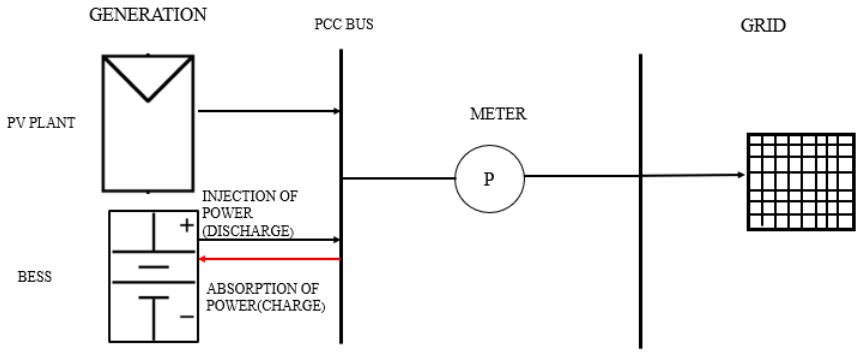

Figure 2.1: Single Line Diagram of the system

The system is based on a Type C solar plant and a battery Type C, both connected to the PCC (Point of Common Coupling), which is the point where the solar plant connects to the electrical grid and where all standards and regulations must be met. The DC/AC inverter has not been represented for both the PV plant and the BESS.

The study will be carried out considering a 15 MW PV plant, as this size requires frequency control and type C requires, which is essential for analyzing battery degradation, while also allowing for capacity firming. The PV plant will be connected to a battery, the size of which will be determined based on the power and energy it needs to supply. Fol-

lowing a power-to-energy ratio of 4, and considering that the battery's nominal power will be 26% of the nominal power of the solar plant to which it is connected, a 4 MW battery has been selected with an energy of 1 MWh. This nominal power value for the battery was chosen based on the model of Vattenfall's wind and solar park in the Netherlands, which sizes its battery at 23% of the nominal power of the plant [18]. Besides, the function of the battery on that project is to enhanced and flatter output power which is similar to our purpose to smooth the peaks using capacity firming and de Moving Average filter. A potential optimization of the battery sizing will not be developed, as it is not the objective of this project.

The location used for this project is Esbjerg, with a latitude of $55,47^{\circ}$ and a longitude of 8.45°. This city is within DK1; therefore, the regulations mentioned previously in the state of the art must be followed.

2.2 General Requirement Specifications

In this project, the system under study consists of a Type C solar power plant integrated with a battery storage system Type C, both connected at the Point of Common Coupling (PCC). The following requirements have been identified for the overall system and its sub-systems:

2.2.1 Response Time and Settling Time

The battery and associated control system must respond to deviations in solar generation and frequency fluctuations within a predefined time frame. For instance, in the Frequency Containment Reserves (FCR) scenario, the battery should activate the first half of the reserve within 15 seconds, while the last half must be supplied in full within 30 seconds at a frequency deviation of ±200mHz. Maximum power has to be supplied for maximum 15 minutes after which the reserve has to be re-established within the next 15 minutes. [6] Similarly, for capacity firming, the battery should compensate for forecast errors, ideally within the 15 minute bidding interval.

2.2.2 Power and Energy Injection and Absorption

The system must be capable of injecting or absorbing a specific amount of power and energy to ensure that the PV plant's output meets grid requirements and the bid made as well. This includes:

- The battery must be able to supply sufficient power and energy to cover the power demand for the FCR. In this case, the maximum values are 4 MW and 1 MWh, as

these are the rated values of the battery. Therefore, when the plant offers to provide FCR, it should not bid values higher than these.

- In the case of capacity firming, there will be a power request, and the battery will contribute up to the maximum of its capacity. If the requested power exceeds what the battery can deliver, it will not be supplied, as the battery will not be capable of meeting the demand.
- When both services are combined, priority will be given to FCR, as it is a mandatory service. Capacity firming will be provided as well, but only if the battery has sufficient remaining capacity after fulfilling the FCR requirements.

2.2.3 Capacity Fade and End of Life(EOL)

The battery degradation will be analyzed based on its capacity fade over time. The end of life (EOL) of the battery is defined as the point when it has lost 20% of its capacity [19].

2.2.4 Operational Scenarios

The system must support different operating scenarios:

- **Capacity Firming:** The battery compensates for fluctuations in the PV output to meet market bids.
- **Frequency Regulation (FCR):** The battery responds to instantaneous frequency deviations.
- **Combined Operation:** The battery performs both functions simultaneously.

These specifications form the basis for evaluating the system's performance and will guide the modeling, simulation, and eventual assessment of battery degradation under various conditions.

2.3 Chapter Summary

This chapter provides a general overview of the single-line diagram of the project, showing the different components involved. Additionally, it explains the various service scenarios that will be carried out, along with the requirements each of them must meet. It also defines the criteria used to consider the end of life of the battery in the lifetime analysis.

Chapter 3

Framework Design

In this chapter, the framework and the implementation of each service will be presented. Specifically, capacity firming, FCR, and the combined services will be described.

In Figure 3.1, the design of the project framework is presented, detailing the inputs from the various models and outlining the workflow. Once the inputs are processed through their respective models and the output from the battery model is obtained (SoC and Power), it will be used to analyze battery degradation and, consequently, its lifetime. Ultimately, these results will be processed and presented for further analysis.

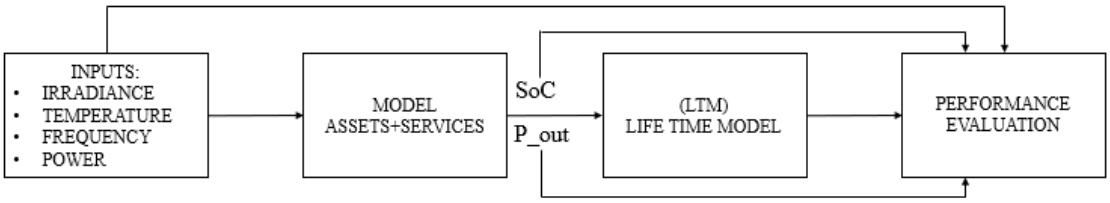

Figure 3.1: Framework Architecture

3.1 Inputs

As shown in Figure 3.1, there are four different inputs.

The data used has been actually measured at a measurement station located at the site, so it consists of real data for the entire year of 2023. The irradiance and temperature are real measurements taken every 10 seconds throughout the year, and the same applies to the frequency, which was measured every 4 seconds for the entire year.

On one hand, irradiance and temperature are inputs to the solar plant model. On the other hand, frequency is the input for the FCR model. Finally, the power obtained from these models serves as the input to the battery model. Power is the only variable that is not directly measured but is instead obtained through the different models.

3.2 Assets & Services

On one hand, the model assets in this project are the PV power plant and the battery. On the other hand, there are three clearly differentiated services: the first is when capacity firming is performed, the second is when the FCR is carried out and the third when both services are combined. Therefore, the different designs that are intended to be implemented are shown below.

3.2.1 Capacity firming

With the actual irradiance and temperature data obtained from a station in Esbjerg over 10 seconds for the entire year of 2023, the power generated will be estimated. The solar plant will have the previously mentioned characteristics. The plant model was created earlier and estimates the output power of the PV plant. The model for estimating the output power will not be developed; instead, the actual irradiance and temperature data obtained will be implemented into that model.

On the other hand, a system will be used to perform the moving average of the output power generated every 10 seconds, allowing us to create the target power in 15-minute intervals, which corresponds to the bidding format in the electricity markets.

Once the target power and the output power of the PV plant are available, the capacity firming will be performed, and it will be possible to see when the battery charges or discharges, depending on whether more or less power is needed. With these charge and discharge cycles, the degradation of the battery will be analyzed using the lifetime model estimation.

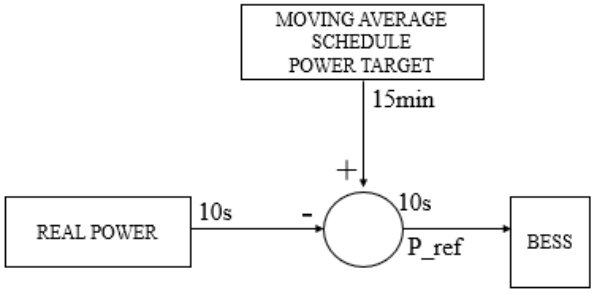

Figure 3.2: Capacity Firming Block Diagram

The following expression aims to show how this capacity firming will work. With the difference between the real power and the target power, it will be possible to see when the battery charges and discharges.

$$\Delta \text{diff}_{\text{Power}} = \text{Power}_{\text{Target}} - \text{Power}_{\text{PV}} \tag{3.1}$$

The previously obtained power data should be input into the battery model to ultimately analyze its degradation.

3.2.2 FCR

The frequency data has been obtained for 4 seconds throughout the year 2023. Following the FCR requirements in DK1, the frequency must be maintained between 49.8 Hz and 50.2 Hz. Therefore, when there are variations, the battery must either supply power or absorb it to stay within this range.

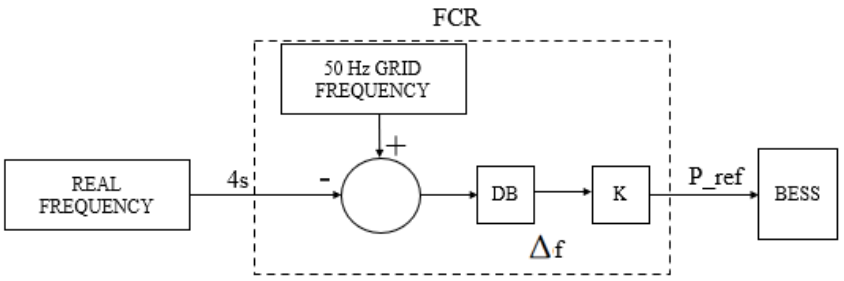

Figure 3.3: FCR Block Diagram

In the following equation, the difference in frequency between the FCR and the actual measured frequency is discussed. Ultimately, this difference must be expressed in power,

which will be absorbed or injected by the battery. These charge and discharge cycles will be analyzed to assess the battery's degradation.

$$\Delta \text{diff}_{\text{Freq}} = 50Hz(\pm 20\text{mHz}) - \text{Freq}_{\text{data}} \tag{3.2}$$

Basically, the operation of FCR is represented by the following equation:

$$P = k \cdot \Delta f \tag{3.3}$$

In this equation, k is the constant representing the slope shown, for example, in Figure 1.3, and Δf is the frequency deviation. Depending on this deviation, the power will vary accordingly. If there is a frequency drop, power will be injected; if there is an over-frequency, power will be absorbed.

3.2.3 Combined Services

Once the FCR and capacity firming models have been developed, each will provide a reference power output from their respective models. The FCR power is generated with a sample time of 4 seconds, while the capacity firming power has a sample time of 10 seconds. Therefore, an interpolation will first be performed to obtain the capacity firming values every 4 seconds so they match the frequency sampling. Once both power vectors are aligned with the same sample time, they will be summed according to certain criteria, which will be presented in the following chapter in section 4.3 and with the flowchart in Figure 4.11.

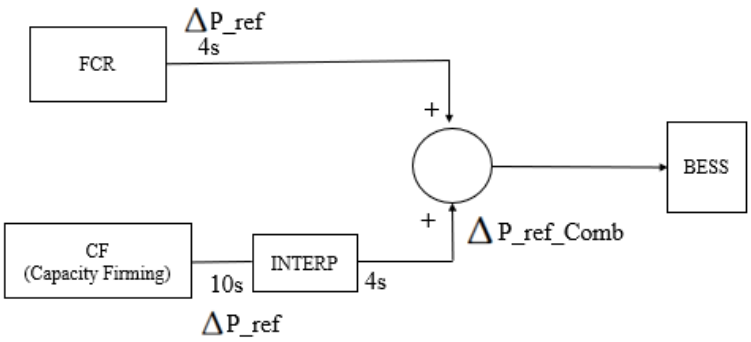

Figure 3.4: Combination of Services Block Diagram

Once the combined power from both models is obtained, it will be used as input to the battery model, which will allow us to obtain the battery's output power and its state of charge (SoC). These results will enable us to analyze its lifetime in the following sections.

3.3 Lifetime Model

In this section of the framework, the battery lifetime will be studied while performing the three different services mentioned previously. The analysis will focus on battery degradation in terms of its capacity loss. For this purpose, the power profile and State of Charge (SoC) are used.

To estimate the capacity loss, two scenarios are analyzed: when the battery is idling (i.e., power equals zero), and when it is cycling. Using equations that model battery capacity degradation, the total degradation is calculated as the combination of both scenarios over the course of one year of service operation.

The degradation obtained for one year will then be linearly extrapolated until a 20% capacity loss is reached, which is considered the end of life of the battery.

3.4 Performance Evaluation

Throughout the project, both the input data and the outputs obtained from the different models are analyzed. This section focuses on evaluating and comparing the results, particularly in terms of battery degradation under each of the provided services. A critical analysis is carried out to interpret the performance, highlight key differences, and discuss the impact of each service on battery lifetime and overall system behavior.

3.5 Chapter Summary

This chapter aims to present the framework to be implemented. It provides a detailed analysis of the three services that will be provided, including their respective block diagrams and how they operate. This analysis is essential to understand how the output power from each model is obtained, which will later be used as input to the battery model in order to generate the corresponding power and state of charge (SoC) profiles.

As shown in the framework diagram in Figure 3.1, once these profiles are obtained, the battery's lifetime under the different services will be studied, followed by a post-processing of the results.

Chapter 4

Framework Implementation

In this section, the designs mentioned in the previous chapter will be implemented to analyze the battery's power profiles in the different scenario services, so that in subsequent chapters, the battery's degradation can be analyzed.

4.1 Inputs for the Capacity Firming Implementation

Firstly, irradiance data was obtained every 10 seconds at a measurement station in Esbjerg throughout the entire year of 2023, as shown in Figure 4.1.

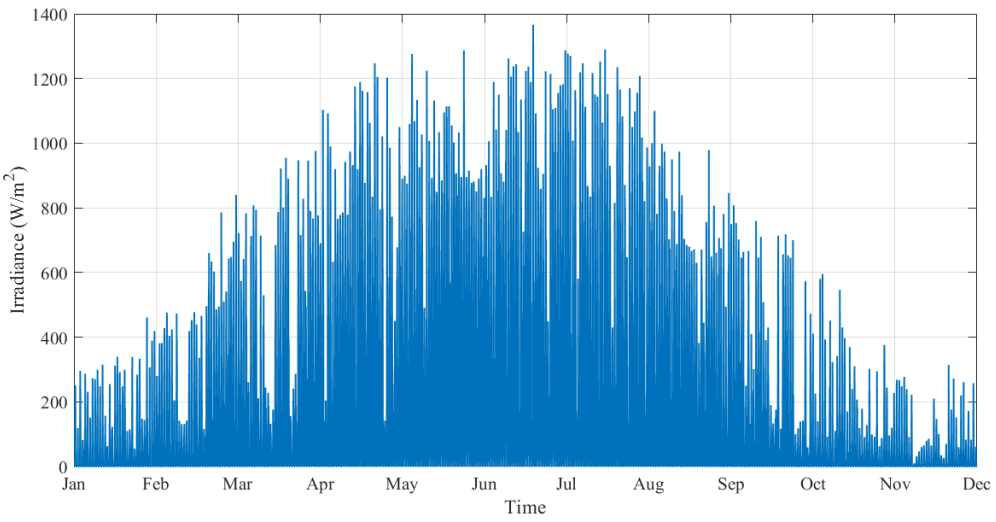

Figure 4.1: Irradiance each 10 seconds during 2023

Once the irradiance data for the entire year has been obtained, it is added to a solar plant model in Simulink, which returns the plant's output power using those irradiance

values and with the plant's capacity defined as 15 MW. This model also considers temperature; therefore, two inputs—irradiance and temperature—are introduced to ultimately obtain the PV plant's output power as it can be seen in the appendix section A.3.

For a representative analysis, the month of July has been selected. This allows for the examination of irradiance levels and the corresponding output power generated by the model. Subsequently, the steps involved in calculating the power difference between the real data recorded every 10 seconds and the 15-minute average power schedule steps values are detailed. As it can be seen in Figure 4.2.

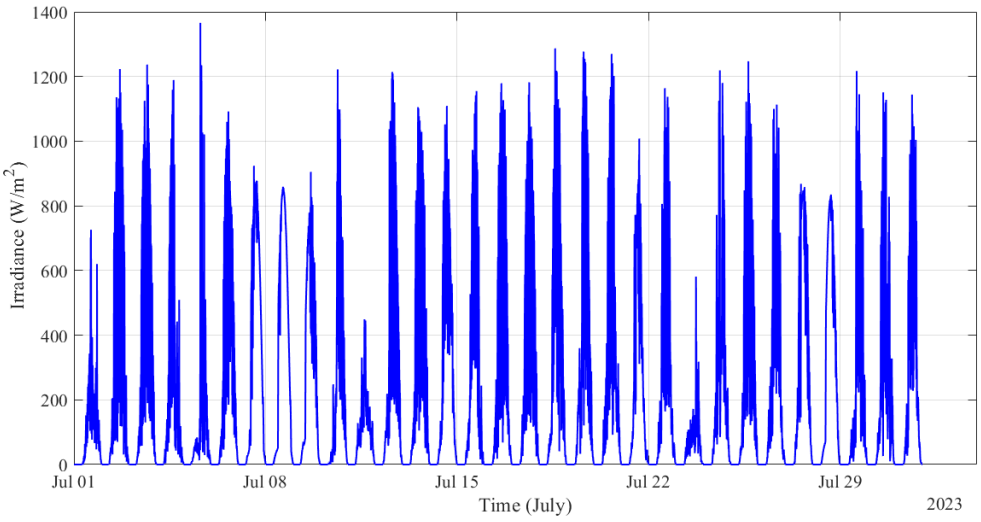

Figure 4.2: Irradiance each 10 seconds during July 2023

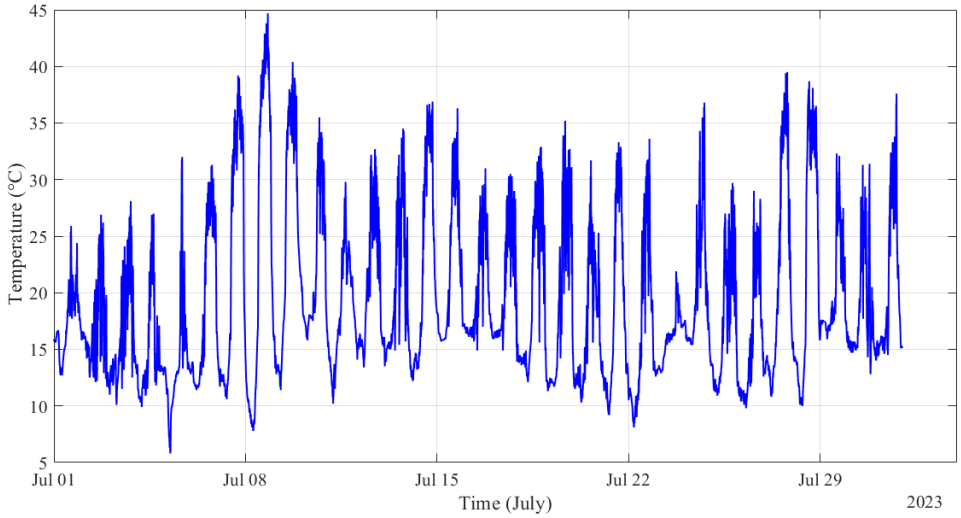

Figure 4.3: Temperature each 10 seconds during July 2023

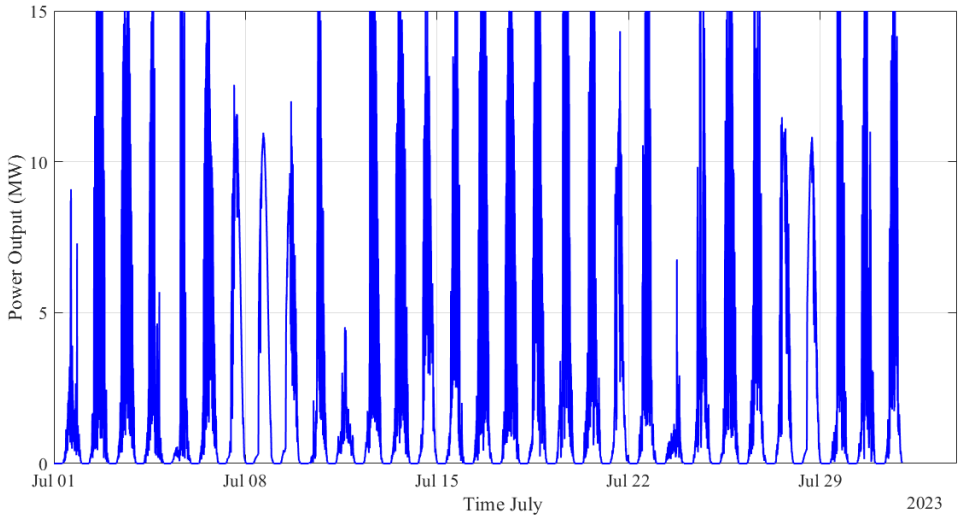

Figure 4.4: Output Power PV plant in July

It is shown as well the temperature during the whole month of July in the Figure 4.3. Once its used the irradiance and the temperature each 10 seconds the whole month of July in the PV model estimator it is obtained the output power of the PV plant during this month. Is it obtained first per unit (pu) and its scaled to the rated capacity of 15 MW as it shown in Figure 4.4.

Once the output power of the solar plant has been obtained, this data is added to a

moving average model, which will create 15-minute steps with that power. This would be the desired input for making offers in the electricity markets. Basically, what is being done is taking a 15-minute data window with data recorded every 10 seconds and averaging them to generate this step. The difference between the real data and this step will determine what the battery needs to absorb or inject, depending on the situation. Besides the MA should smooth the peaks[20].

In Figure 4.5, a zoomed-in view has been provided to better visualize the generated schedule power steps and how the actual power data recorded every 10 seconds compare to these steps.

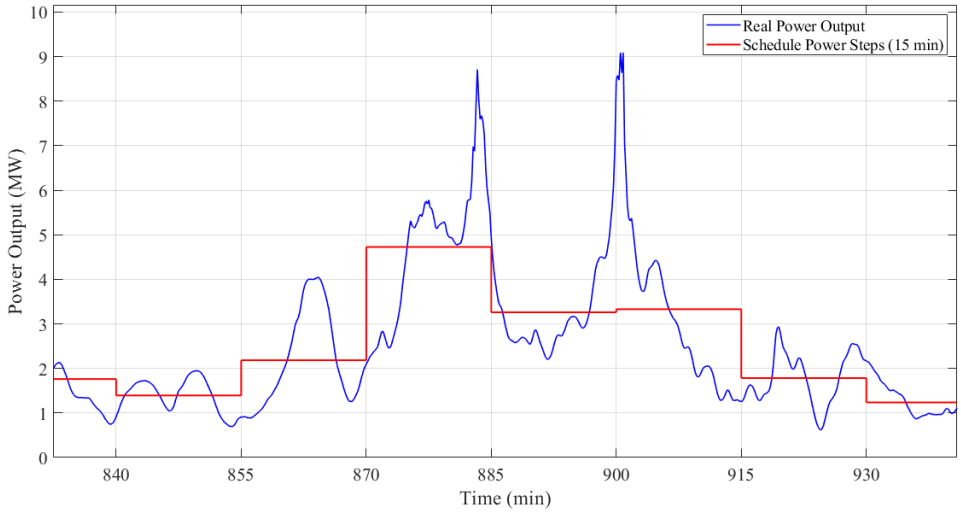

Figure 4.5: Steps 15 minutes in July

Finally, the output power is compared with these steps, and the difference between them will be the power request to the battery to perform capacity firming. The difference between the real data and the schedule power steps is shown in Figure 4.6.

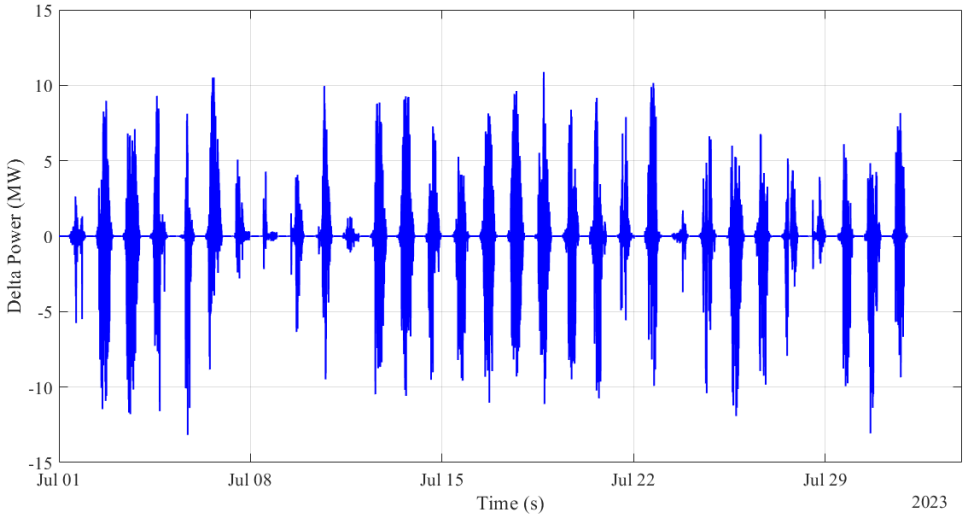

Figure 4.6: Difference of power between schedule steps and real data

In Figure 4.6, you can see how the power was obtained by comparing the schedule power steps generated by the Moving Average model with the actual power measured every 10 seconds.

4.2 Inputs for the FCR Implementation

Frequency data was obtained every 4 seconds throughout the entire year of 2023, as shown in Figure 4.7.

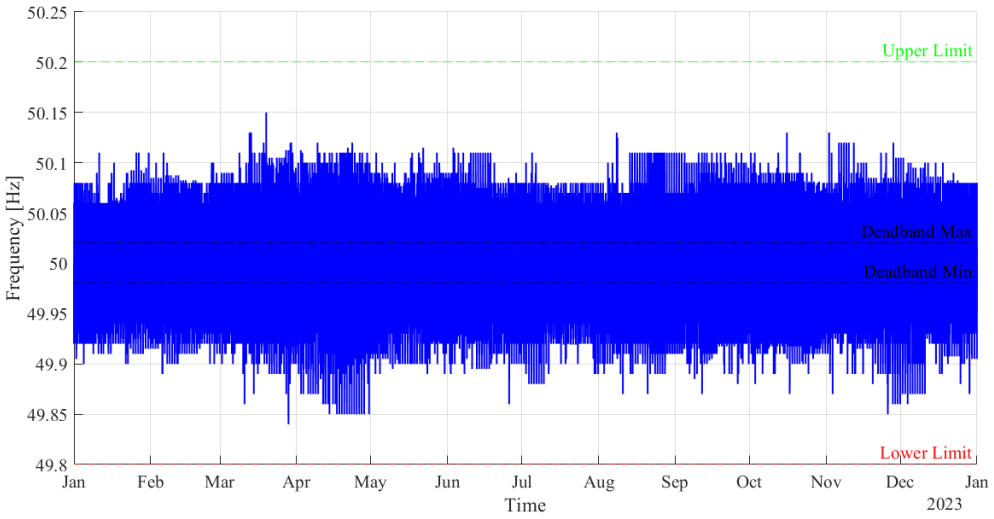

Figure 4.7: Frequency each 4 seconds during 2023

Once the frequency data for the entire year has been obtained, it is necessary to analyze when the frequency is below or above 50 Hz, as this will determine whether the battery power profile (charges or discharges). Therefore, the Figure 4.7 shows the deadband within which the frequency can remain without variations and the maximum and minimum limits to which the frequency can deviate. Values outside the deadband must be corrected.

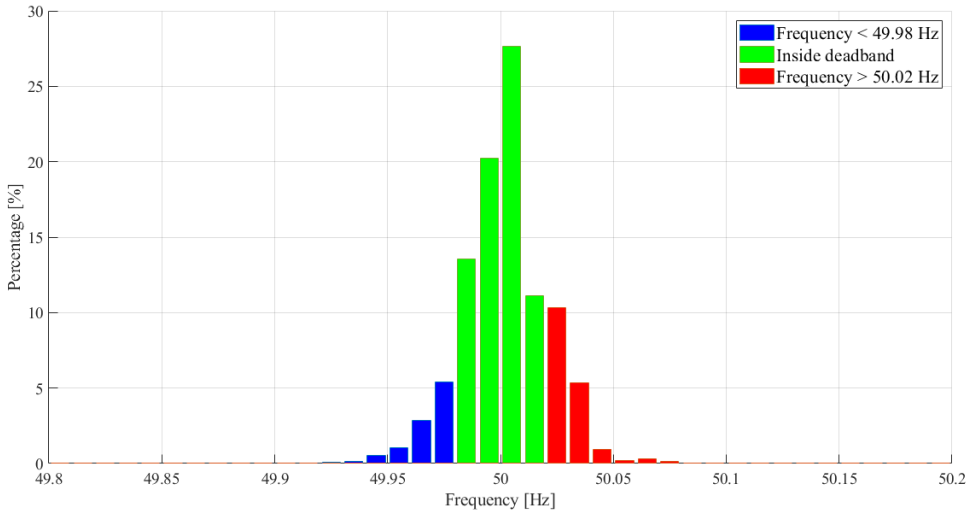

Figure 4.8: Frequency above, below and inside of the deadband margin

As shown in Figure 4.8, the frequency data above, below and inside the deadband have

been analyzed and displayed in the form of a histogram, showing the data of the whole year 2023.The bin width of the histogram it has been displayed in 10 mHz. With this data, the power that the battery will inject or absorb must be obtained. To clarify the amount of frequency in each interval—whether it falls within the deadband, above, or below—it is shown in Figure 4.9 the percentage of each over the course of one year. This is important because in Figure 4.8, it might give the impression that there are more or less the same under-frequency events than over-frequency ones, but that is not the case. In fact, there is a slight predominance of over-frequency occurrences over time.

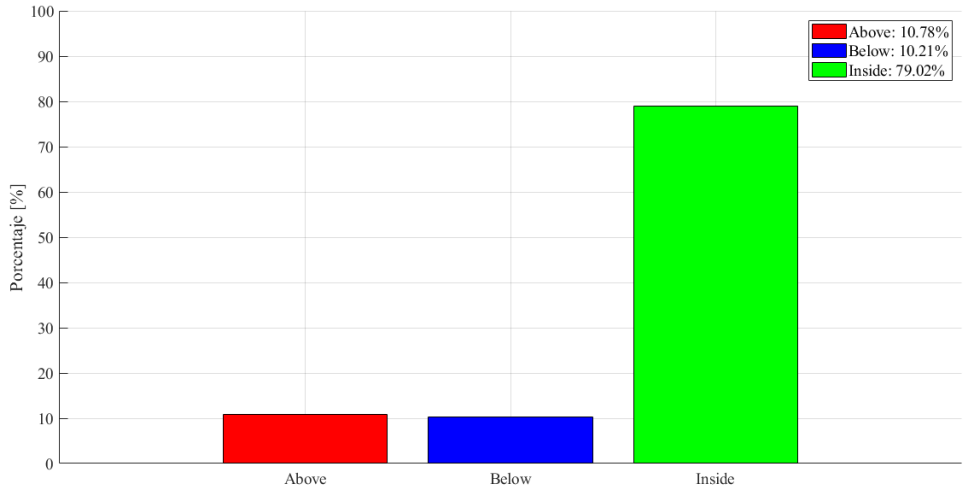

Figure 4.9: Frequency total amount in percentage

In Figure 4.10 it is shown the frequency each month for the whole year 2023 in a boxplot. The purpose of this image is to show the values within the deadband as well as those outside of it, both above and below, for each month.

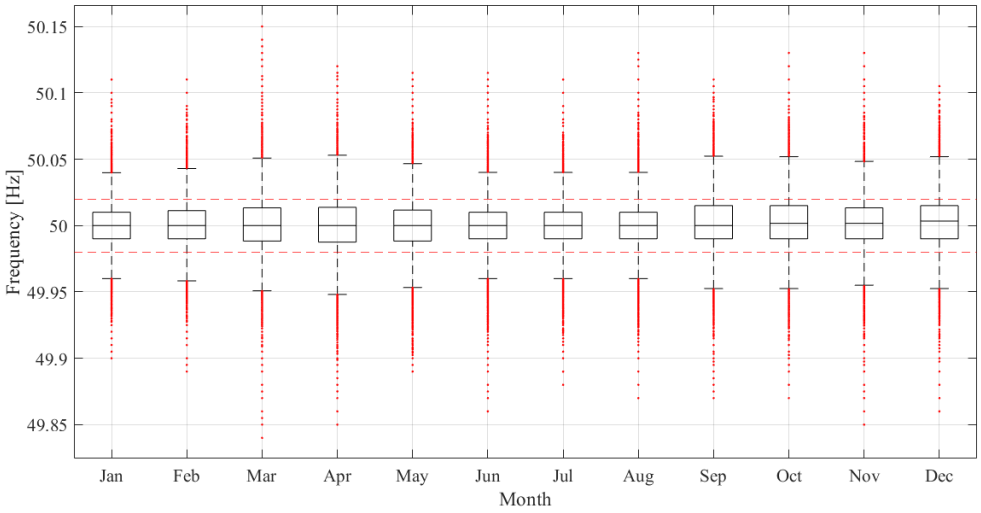

Figure 4.10: Boxplot of year 2023

The boxplot shows that most boxes lie within the deadband, indicating that a large portion of the frequency values fall within these margins. The minimum and maximum deadband limits are marked with red dashed lines in the figure. This observation aligns with Figure 4.8, which shows a high concentration of values within the deadband range. Additionally, the relatively short whiskers suggest low variability in most months. However, in March, the whiskers are noticeably longer, indicating greater dispersion during that month.

4.3 Inputs for the Combined Services Implementation

As previously mentioned in subsection 3.2.3, once the output powers from the respective models for the different services are obtained, the capacity firming power is interpolated to match the 4-second sample time of the FCR service. The power outputs from these services serve as inputs to the model when the two services are combined. The combination of these two power signals follows specific criteria, as shown in the flowchart in Figure 4.11.

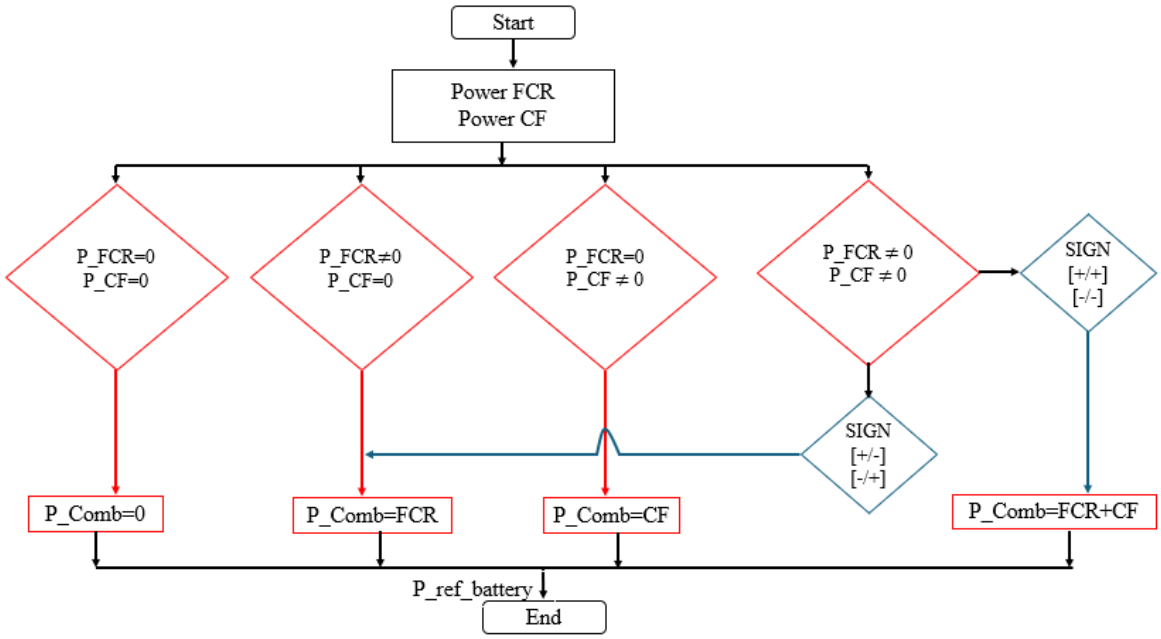

Figure 4.11: Flowchart for combined implementation of power references in both services

This flowchart shows in red the four possible conditions that can arise when combining the power outputs from the two different services. Priority is given to the FCR service, as it is a mandatory requirement, and if possible, the capacity firming service is also fulfilled. The most challenging condition, in which priority is clearly given to FCR, occurs when both services request non-zero power.

In blue, the flowchart distinguishes between the two possible scenarios: when both power signals have the same sign and when they have opposite signs. If the signs are opposite, priority is given to the FCR service (regardless of the sign), since the battery cannot charge and discharge simultaneously while fulfilling both service requirements. If the signs are the same, the power signals are summed, and the battery model will subsequently limit the total power to what the battery can actually deliver.

4.4 Battery Model Implementation

Once the capacity firming and FCR models have been defined to obtain their respective output power, this power should be used as the input to the BESS model. The output of this model will provide the power and the SoC (%), once is obtained, the battery degradation should be calculated during idling operation and battery power is zero and during cycling operation, that is, throughout the charge and discharge processes. It should be noted that the battery model does not follow the established sign convention. Instead,

a negative power signal means that the battery is charging, and a positive power signal means that the battery is discharging. Therefore, both the capacity firming model and the FCR model will follow this sign convention.

The entire battery model is explained in detail in Section A.2 in the appendix. Therefore, here it will be shown the battery's output power profile and its SoC throughout the year 2023 when performing capacity firming.

The following will show the power request profile, the output power profile, and the state of charge obtained from the capacity firming. In Figure 4.12 is shown the power request made to the battery throughout the year 2023 offering the capacity firming service. This comes from the difference obtained between the real data and the moving average model.

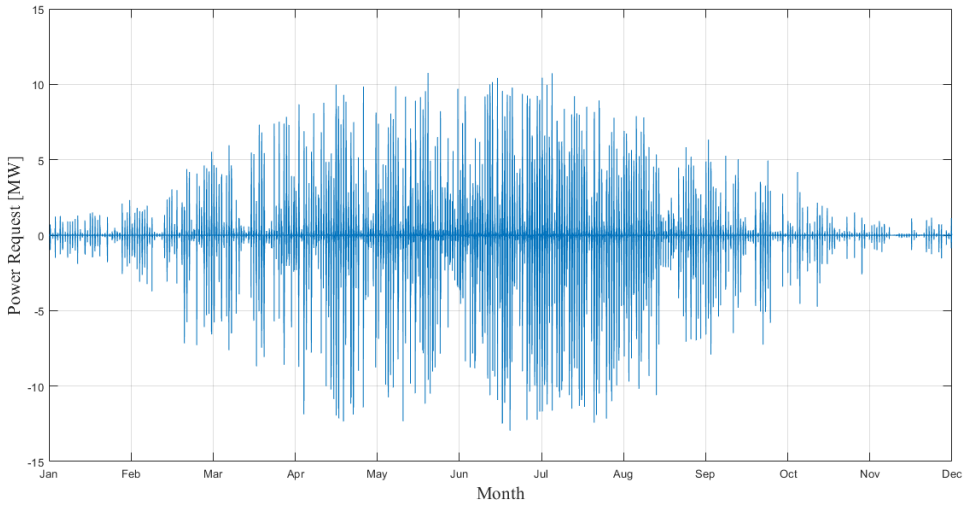

Figure 4.12: Requested Power 2023

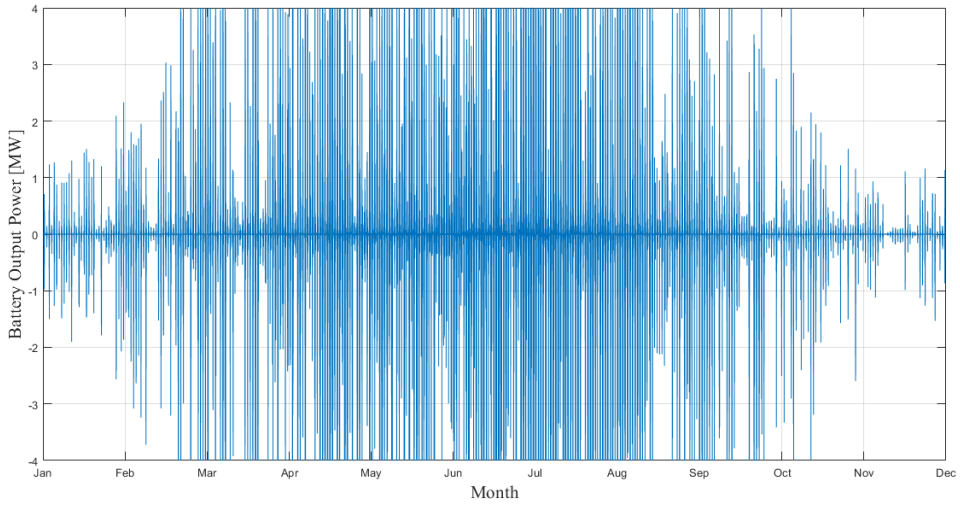

Figure 4.13: Battery Output Power Performing Capacity Firming

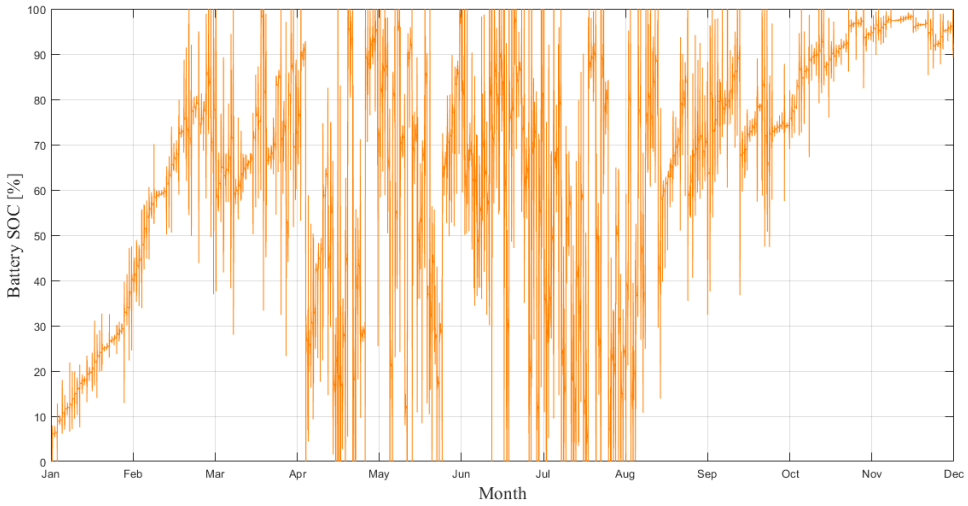

Figure 4.14: Battery State-of-Charge Performing Capacity Firming

As can be seen, there are large peaks of up to 13 MW in the power request.

The Figure 4.13 shows the output power that the battery can provide. In this case, the battery has a power of 4 MW, and as can be observed, the power is limited within these limits ±4.
In Figure 4.14, the state of charge profile of the battery throughout the year 2023 can be

seen. Both the output power shown in Figure 4.13 and Figure 4.14 will be used in the following chapter to calculate the battery degradation.

On the other hand, the output power and state of charge profiles during the FCR operation have been obtained, as shown in Figure 4.15 Figure 4.16.

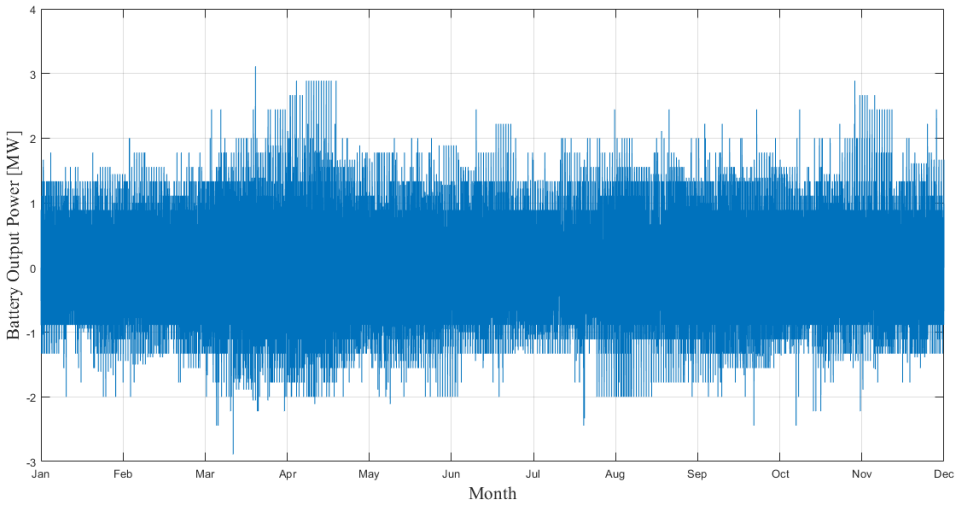

Figure 4.15: Battery Output Power Performing FCR

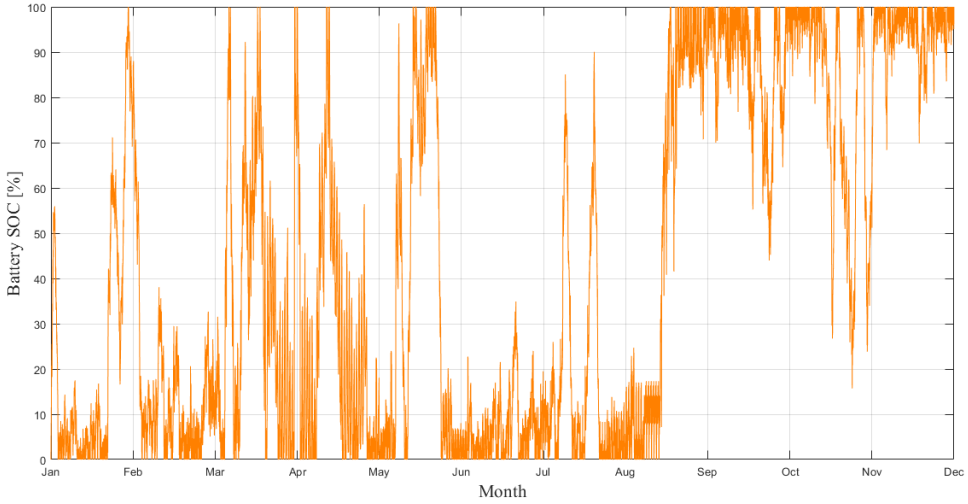

Figure 4.16: Battery State-of-Charge Performing FCR

It can be seen that both images are different compared to those from the model when

capacity firming was performed. Further research and analysis will be carried out in the next chapter.

In Figure 4.17 and Figure 4.18 it is shown the power output and the State of Charge (SoC) profile obtained from the battery model when performing both services simultaneously.

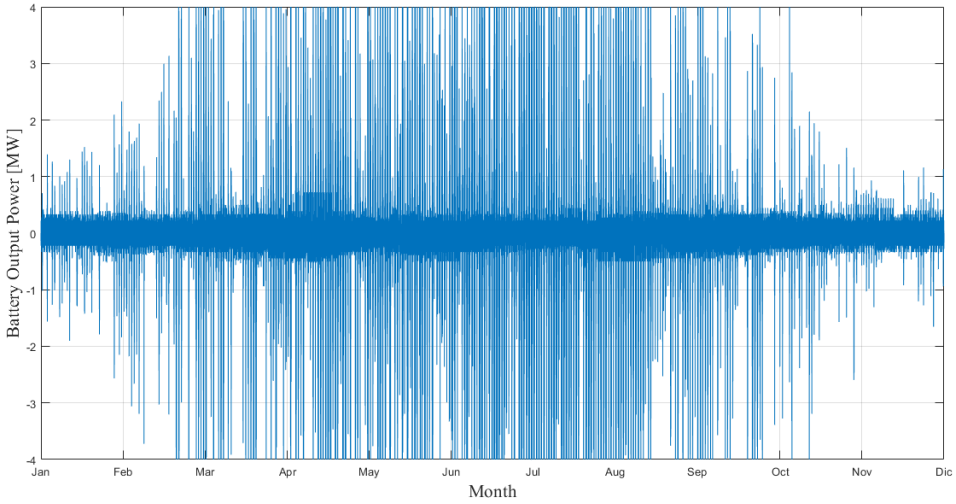

Figure 4.17: Battery Output Power Performing Combined services

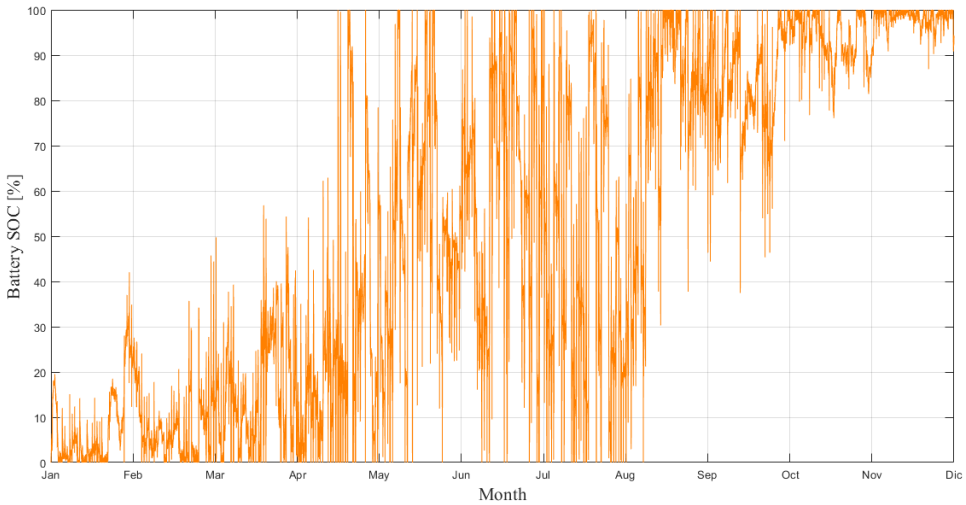

Figure 4.18: Battery State-of-Charge Performing Combined services

4.5 Chapter Summary

In this chapter, the inputs of the different services within the framework have been analyzed. Their performance within the respective models and under the different services has been assessed, resulting in the reference output powers for each model. Subsequently, the power and state of charge (SoC) profiles of the battery have been obtained for each scenario, which will serve as the basis for the battery lifetime analysis in the next chapter, where each service will be evaluated individually.

Chapter 5

Assessment Studies of Battery Lifetime Model

In this chapter, the battery degradation under the previously mentioned scenarios will be presented: when capacity firming is performed, when FCR is used, and when both are combined.

5.1 Case Study 1: Capacity Firming

In this scenario, the aim is to analyze the battery degradation during capacity firming, as explained in previous chapters. Using the battery model, the power and state of charge profiles during this scenario have been obtained, which are then used to calculate the battery degradation.

To calculate the battery degradation, two operating conditions must be considered.[16] [19].

First, the degradation when the battery is in idling mode has been analyzed. For this, the power and state of charge profiles have been examined to identify the periods when the power is equal to zero. Once these periods were obtained, they were grouped into intervals of 10%, meaning that if at any moment the battery is at zero power and a state of charge of 7%, it is considered as 10%. Therefore, there will be groups from 10% to 100% state of charge, resulting in 10 groups, each covering a 10% range. The total number of hours the battery remains in idling during this year is 4127.75 hours, while the total number of hours in a year is 8760, meaning that the battery is in idling mode for 47.1% of the time during that year.

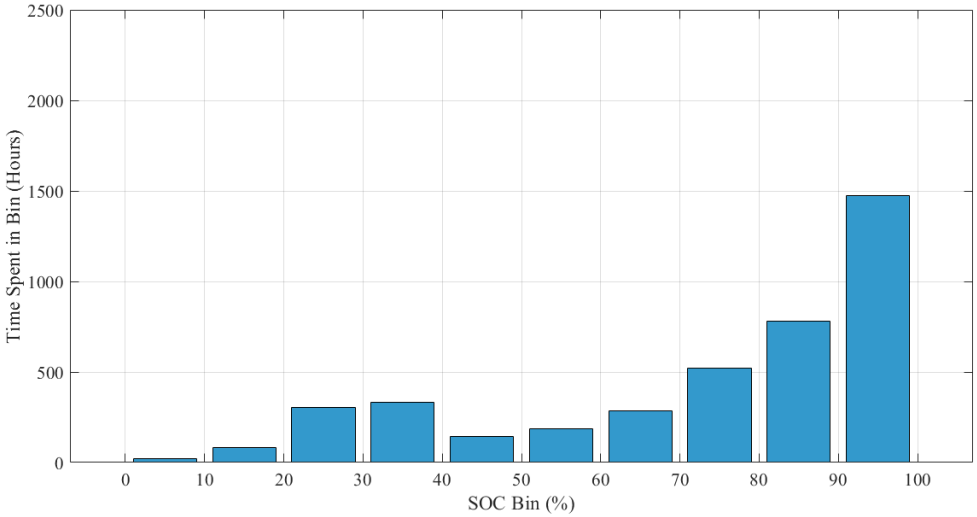

Figure 5.1: SoC distribution during idling operation for capacity firming service

This histogram shows the number of hours the battery remains idle. It can be observed that the most predominant bin corresponds to a state of charge (SoC) of 100% at zero power, indicating the battery idles when fully charged.

To calculate the degradation during idling, the Equation 5.1 has been used[16]:

$$C_{\text{f,cal}} = 0.1723 \cdot e^{0.007388 \cdot \text{SoC}} \cdot t^{0.8} \tag{5.1}$$

The degradation during idling is expressed as $C_{\text{f,cal}}$, where the subscript "cal" refers to calendar aging. The term $e^{0.007388 \cdot \text{SoC}}$ accounts for the effect of the state of charge (SoC) on the degradation, meaning that higher SoC values lead to faster degradation. The factor $t^{0.8}$ represents the time dependence of the degradation process. The constant 0.1723 is a scaling factor derived from empirical data, adjusting the degradation rate accordingly. It was found the degradation due to calendar aging performing the capacity firming was 1.7917% in one year.

Second, it has been calculated the degradation when the battery is cycling. The Equation 5.2 has been used[16]:

$$C_{\text{f,cyc}} = 0.021 \cdot e^{-0.01943 \cdot \text{SoC}} \cdot cd^{0.7162} \cdot nc^{0.5} \tag{5.2}$$

In this equation, $C_{\text{f,cyc}}$ represents the capacity fade due to cycling. The term $e^{-0.01943 \cdot \text{SoC}}$ accounts for the effect of the average state of charge (SoC) during the cycle, indicating that a higher SoC results in a faster degradation rate. The factor $cd^{0.7162}$ represents the effect of the cycle depth (cd), meaning that deeper cycles lead to a higher degradation rate. Finally,

the term $nc^{0.5}$ accounts for the number of cycles (nc), showing that degradation increases with the number of cycles. To obtain these values, the power and SoC profiles were sent through a rainflow cycle counting algorithm to determine the different terms for the equation.

Once the number of cycles, the depth of these cycles, and their average SoC have been obtained, they are displayed below in a 3D plot with a resolution of 5%. It was found that the degradation caused by cycling operation over one year is 2.1186%. This value is slightly higher than the degradation caused by calendar aging, which is consistent with the fact that during that year the battery spent more time cycling than idling.

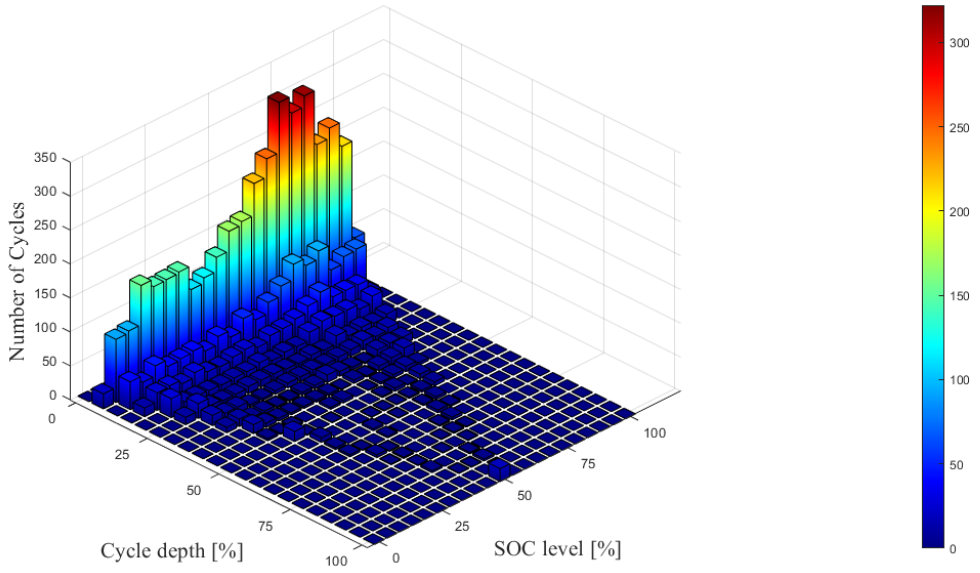

Figure 5.2: Distribution of cycles according to their cycle depth and average SoC during capacity firming

Once the degradation in calendar and cycling is obtained, a linear extrapolation is performed until a 20% degradation is reached, which is considered the EOL (End of Life) of the battery. As it shown in the Figure 5.3. Performing a linear extrapolation simulates the worst-case scenario, as it assumes that degradation will be the same each year. However, this does not necessarily hold true, and as shown in various studies analyzing battery capacity degradation, the behavior is not linear and tends to decrease over the years.[16][19][21].

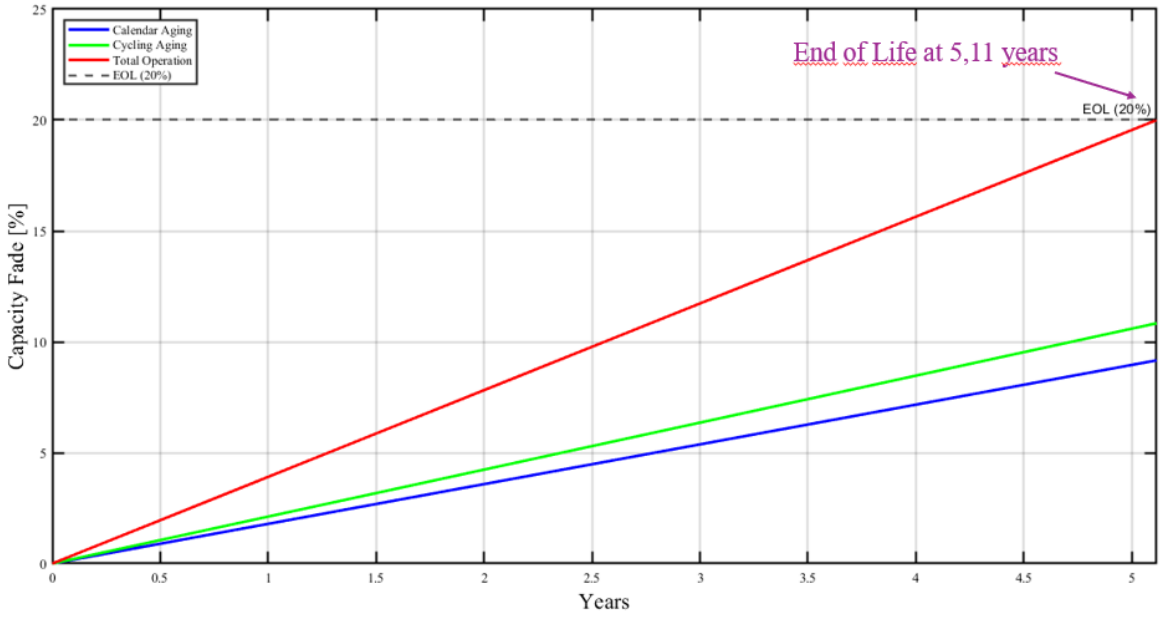

Figure 5.3: Capacity fade while battery is performing capacity firming

It was found that the battery performing capacity firming under these conditions has an estimated lifetime of 5.11 years, reaching a 20% degradation in its capacity.

5.2 Case Study 2: FCR

As previously explained in section 5.1, the same procedure will be followed for this case study. First, the battery degradation during idling operation will be obtained, and then during cycling operation.

When the battery has been analyzed during idling operation, the Figure 5.4 has been obtained:

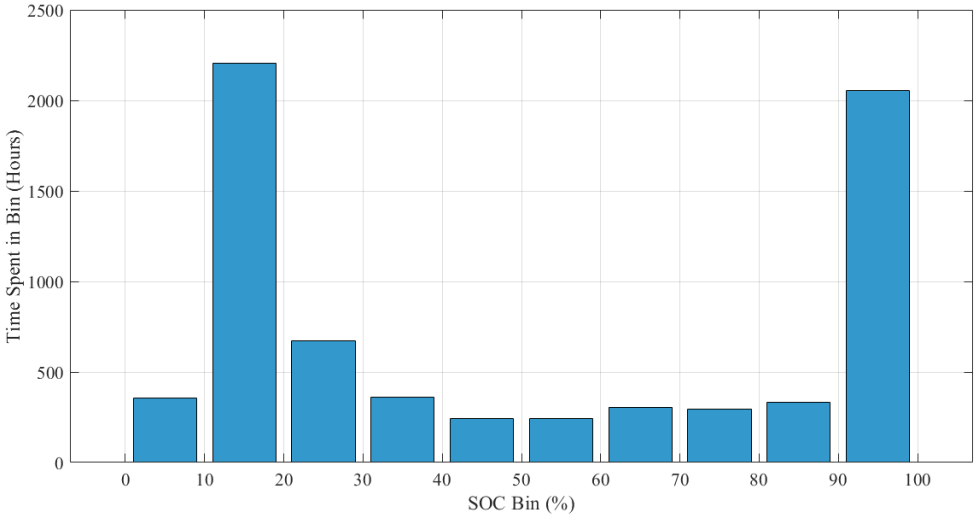

Figure 5.4: SoC distribution during idling operation for FCR service

In this case, a significant difference can be observed compared to when the battery was operating in idling mode while performing capacity firming. Now, while performing FCR, the total amount of time spent in idling operation over the year is 7070.12 hours, which means that the battery remains at zero power for 80% of the time, and during the remaining 20% of the time it is in cycling operation. This can also be observed earlier in the histogram Figure 4.8, where it is shown that the frequency remains within the deadband. As a result, no action is taken, and the power stays at zero. Another difference compared to the previous case lies in the distribution of the SoC. In the previous scenario, during capacity firming, the battery remained at 100% SoC for a significant amount of time—around 1500 hours. In this case, although the total time at 100% SoC is even higher (2100 hours, 23.97% of the total time in one year), the predominant SoC value is 20%, with a total duration of approximately 2200 hours being 25.11% of the total time in one year. This implies less degradation, as expressed in Equation 5.1, because lower SoC values lead to reduced degradation. Nevertheless, the considerable time spent at 100% SoC will still contribute to higher degradation.

To calculate the battery degradation, the previously used formula shown in Equation 5.1 was applied. In this case, it was found that the degradation due to calendar aging when performing FCR is 2.4335%, which was expected, since the battery spends the vast majority of the time in idling operation. Therefore, a higher calendar degradation is obtained during FCR operation compared to capacity firming.

Subsequently, following the previous procedure, the degradation due to cycling operation was analyzed using the Equation 5.2. In this case, the degradation due to cycling

was found to be 0.9234%, which is considerably lower than that observed during capacity firming. This result is reasonable since a battery performing FCR is only cycling for 20% of the total time in a year. Additionally, a 3D map was plotted showing the number of cycles, depth, and average SoC. In this case, a 5% resolution is maintained and it is shown in Figure 5.5.

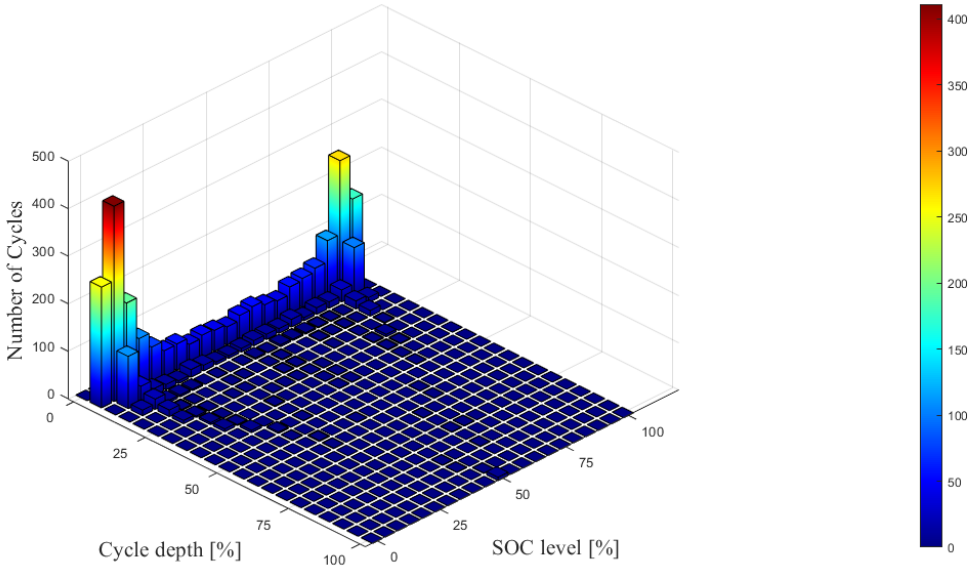

Figure 5.5: Distribution of cycles according to their cycle depth and average SoC during FCR

Following the previous procedure, once the degradation due to calendar and cycling aging is obtained, a linear extrapolation is performed until a 20% degradation is reached, which is considered the EOL (End of Life) of the battery. As shown in Figure 5.6.

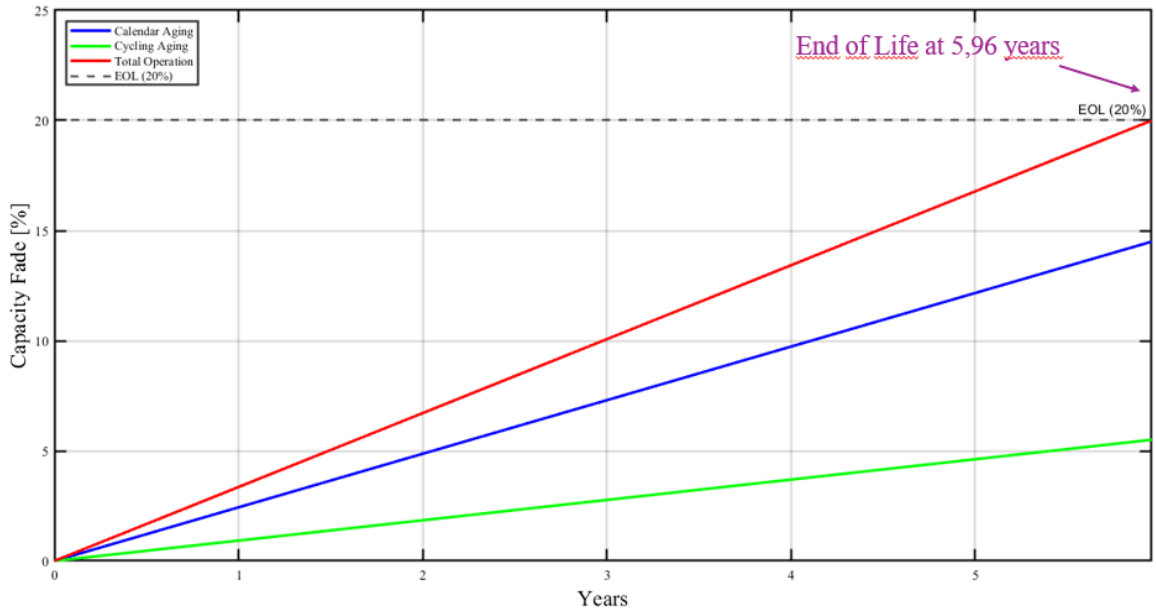

Figure 5.6: Capacity fade while battery is performing FCR

In this case, when compared to Figure 5.3, it can be observed that the degradation due to calendar aging is greater than that caused by cycling. The battery is projected to reach its End of Life (EOL) after 5.96 years under FCR operation, compared to 5.11 years when performing capacity firming. This suggests that the battery is more significantly affected by cycling during capacity firming. This increased degradation can be attributed to the parameters discussed previously: the number of cycles, the average state of charge (SoC), and the cycle depth, as illustrated in Figure 5.2. While the cycle depth distribution is comparable to that shown in Figure 5.5, the average SoC is higher during capacity firming. Furthermore, the number of cycles is also notably greater in the capacity firming scenario, contributing to the accelerated degradation.

5.3 Case Study 3: Combined Case 1 and Case 2

In this section, the degradation analysis of the battery will be carried out when performing the two previously described services: FCR and capacity firming. The procedure will follow the same approach as in the previous cases. The power and state of charge (SoC) profiles have already been obtained, as shown in Figure 4.17 and Figure 4.18.

Using the power profile, an initial analysis is conducted to identify when the battery is in idling operation—that is, when the power is zero—and to determine the corresponding SoC levels during these idle periods. This analysis is presented in Figure 5.7.

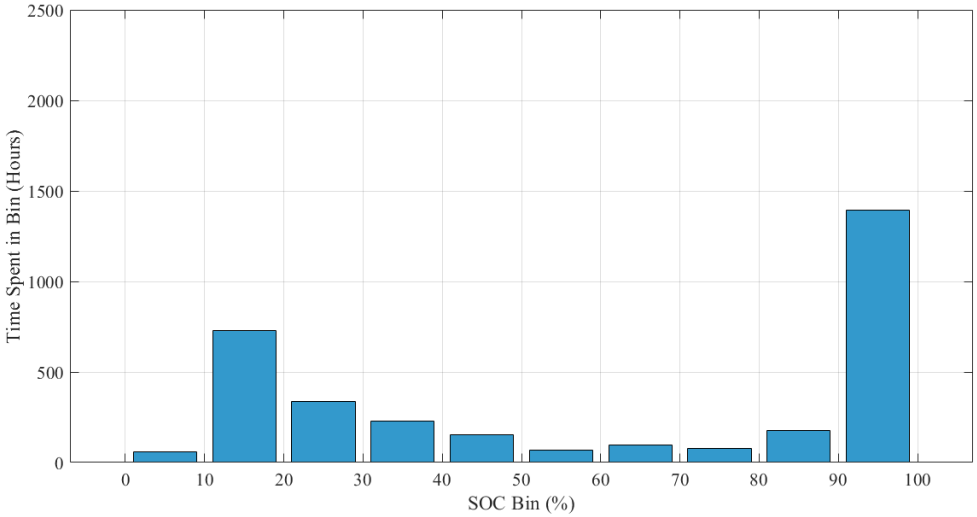

Figure 5.7: SoC distribution during idling operation for combined service

The histogram illustrates the number of hours the battery operates in idling mode. When both services are combined, the battery remains idle for a total of 3313.94 hours, representing 37.8% of the total annual operation time. This highlights periods in which neither service requires power from the battery.

Compared to the individual services analyzed previously, the battery spends less time at zero power in this combined case, with a predominant occurrence of idling at an SoC of 100%.

The degradation due to calendar operation has been calculated using the previously mentioned formula Equation 5.1, resulting in a degradation of 1.3625% during one year.

This value is consistent with the results shown in Figure 5.7, and with the comparison to the other two services. In this scenario, the battery spends fewer hours at zero power. Since idling time is reduced, the calendar degradation of the battery is also lower compared to the other two services.

A 3D plot has been generated to display the number of cycles, their cycle depth and the average state of charge (SoC).

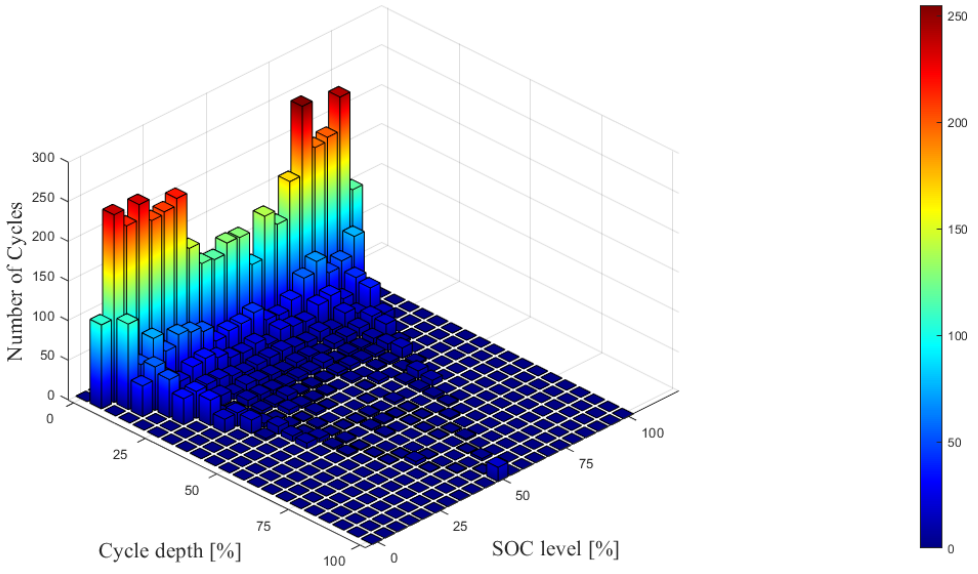

Figure 5.8: Distribution of cycles according to their cycle depth and average SoC with combined services

In this scenario, where both services are combined, a degradation due to cycling of 2.1932% has been obtained, which is slightly higher than that observed during capacity firming. This scenario clearly illustrates how the three main parameters influencing degradation due to cycling operation come into play. In this case, the battery cycles for 5446 hours, compared to 4633 hours in the capacity firming scenario. Despite operating 813 hours longer in this service, the increase in degradation is minimal—only 0.0746%. This highlights how, although the battery cycles for a longer duration, the number of cycles is lower, and the average state of charge (SoC), although reaching high values, also spends a significant amount of time at low average SoC levels.

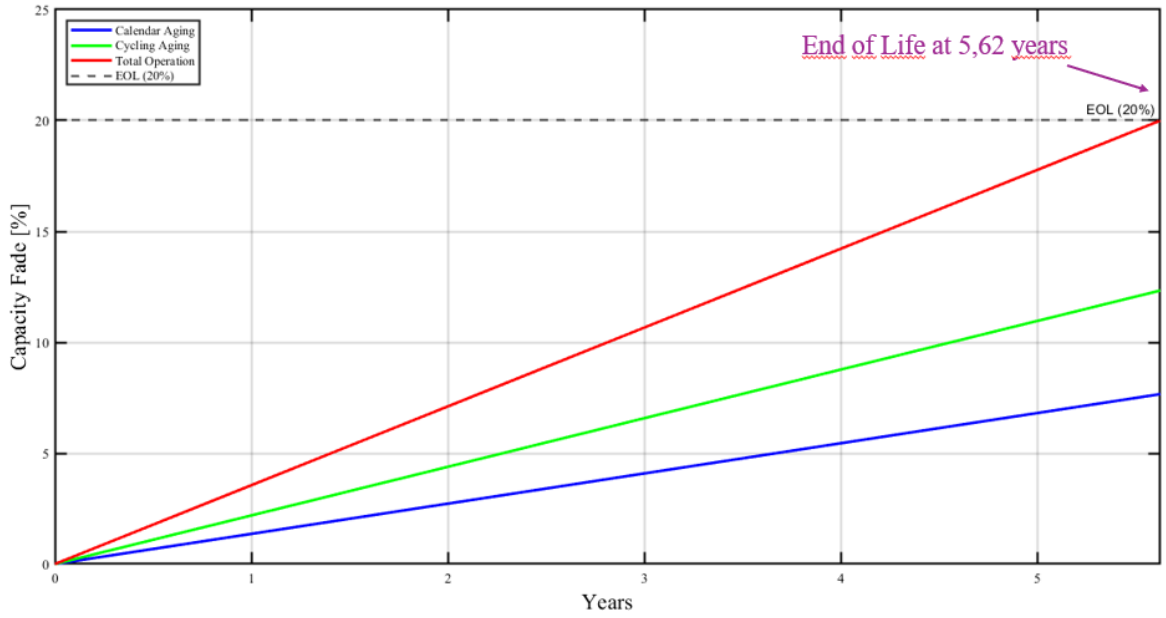

Figure 5.9: Capacity fade while battery is performing combined services

In Figure 5.9, the capacity fade of the battery until it reaches its end of life is shown. In this scenario, where both services are combined, it was found that the battery would last 5.62 years.

5.4 Result analyses

This section aims to present a summary of the results in a more unified and clear manner. Therefore, the total time that the battery remains in idling mode over the course of a year for the three different services is first presented, as shown in Figure 5.10. It can be clearly observed that the battery, when performing FCR, remains in idling mode for a large part of the year, whereas in the capacity firming and combined services scenarios, the idling time is significantly lower. In the case of combined services, it is a mixture of both service profiles, meaning there is a total of 3313 hours in which both services simultaneously request zero power. The following histogram shows the total time each service spends in idling mode, expressed as a percentage.

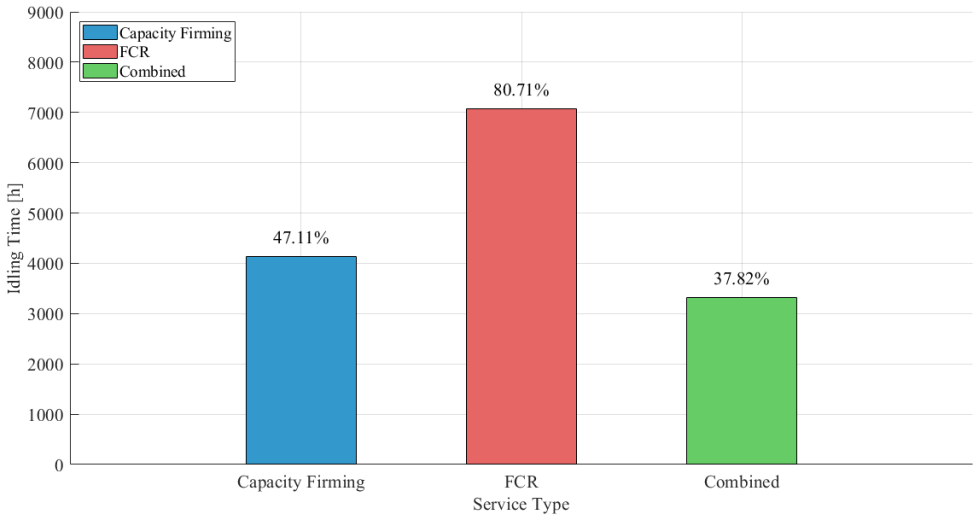

Figure 5.10: Total Time Idling Operation

Following the same procedure used to obtain the previous results, a combined histogram is presented showing the time the battery remains in idling mode, along with the corresponding distribution of SoC in percentage. The SoC values are grouped into bins of 10% intervals up to 100%, as shown in Figure 5.11.

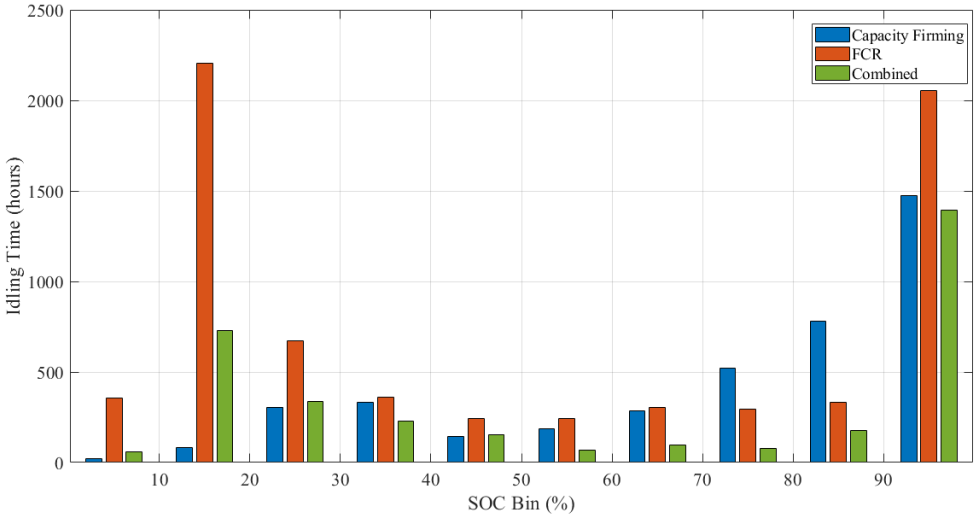

Figure 5.11: Total Time Idling Operation at different SoC

As previously mentioned, this histogram clearly shows that during the FCR service, the battery predominantly remains in idling mode. This histogram provides additional

information, as it also indicates the SoC % at which the battery was idling. These data are relevant since calendar degradation is influenced by the SoC value, as shown in Equation 5.1.

Figure 5.12 shows the total time over one year that the battery is operating in cycling mode.

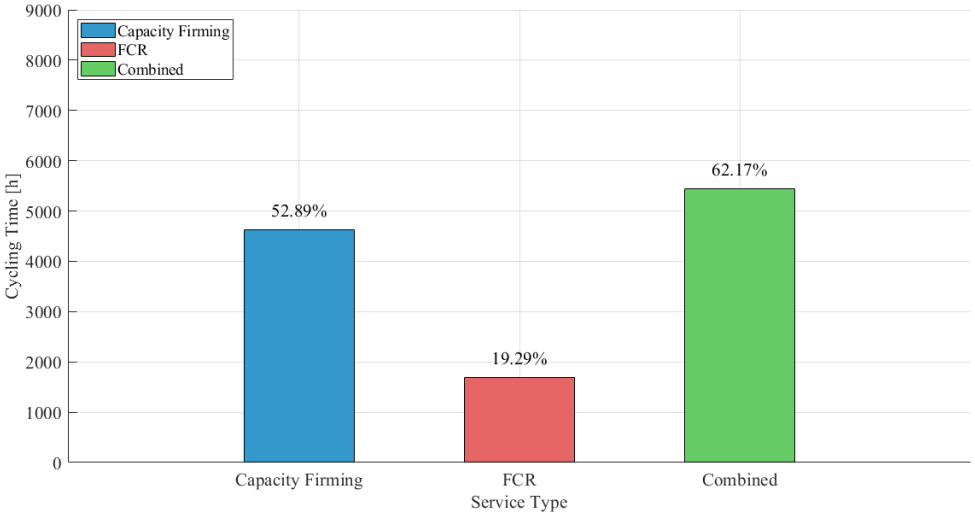

Figure 5.12: Total Time Cycling Operation

In the case of FCR, it is reasonable that the battery cycles for so few hours since it spends a significant amount of time in idling, as shown in Figure 5.10. For capacity firming, more time is spent cycling than idling, and the same applies to the combined services scenario. In the combined case, the battery spends the most hours cycling. This is because it cycles to meet the requirements of FCR and, when possible, those of capacity firming.

Table 5.1 presents all the degradation data due to calendar and cycling aging, as well as the number of years until the battery reaches its end of life for the three different services under study.

	Capacity Firming	**FCR**	**Combined Services**
Calendar Degradation [%]	1.7917	2.4335	1.3625
Cycling Degradation [%]	2.1186	0.9234	2.1932
EOL [Years]	5.11	5.96	5.62

Table 5.1: Battery degradation and estimated end of life under different service scenarios

It can be observed that the most demanding service, and the one that causes the greatest degradation, is capacity firming, while the least degrading is FCR.

At first glance, one might assume that combining both services would lead to higher degradation, as the battery would be fulfilling both requirements. However, this is not strictly the case. When the two services are combined, the battery must meet the FCR requirements, and capacity firming is only pursued when the battery's conditions allow it. It may also be due to the fact that the battery spends less time in idling mode when performing combined services compared to capacity firming alone, and therefore experiences less degradation caused by calendar aging.

In this scenario, the battery's end of life lies between that of the two individual services. This indicates that the battery consistently performs FCR, and partially fulfills capacity firming. If it were fully meeting both services, the end of life would be shorter than that observed for capacity firming alone.

5.5 Chapter Summary

In this chapter, the degradation of the battery was analyzed under the three services described in the previous sections. For each service, the number of hours the battery idles and the corresponding state of charge (SoC) were first presented, followed by the calculation of degradation due to calendar aging. It was observed that the highest degradation during idling mode occurs when the battery performs the FCR service, resulting in a capacity loss of 2.4335% during the first year. In contrast, when both services are combined, the battery spends less time in idling mode, leading to the lowest degradation due to calendar aging among the three scenarios, with a value of 1.3625%.

Subsequently, the degradation due to cycling operation was computed, and a 3D diagram was used to represent the three parameters that most significantly influence cycling degradation: the number of cycles, the depth of the cycles, and the average SoC. The highest degradation due to cycle operation occurs when both services are combined, as the battery spends more time in cycling mode compared to the other two services. In this case, the degradation reached 2.1932%, followed by the capacity firming service with 2.1186%. The lowest degradation was observed during FCR operation, as the battery spent only 19.29% of the time cycling.

This analysis enabled a comparison of the different services and provided insights into how each service affects battery degradation. The End of Life (EOL) of the battery is reached earliest under capacity firming, at 5.11 years, followed by the combined services at 5.62 years, and lastly under FCR, with the longest lifetime of 5.96 years.

Chapter 6

Conclusion & Future Work

6.1 Conclusions

This project aimed to analyze the lifetime of a battery hybridized with a solar plant while performing different grid services. By determining the battery lifetime under each service, a more accurate economic assessment can be carried out. Understanding the battery's lifetime is crucial, as it is one of the most expensive assets in such projects. Knowing how it degrades under different operating conditions allows for the optimization of its usage, ultimately improving the overall viability of the project. This information is particularly valuable for the owners of the solar plant.

The most important conclusions of this master thesis can be summarized as follows:

- When analyzing the temperature and irradiance inputs, their variability due to cloud cover can be observed, which ultimately leads to sudden increases and decreases in power over time.
- By analyzing the frequency data over a year, it was found that during 2023 the values did not vary significantly, with 80% of the frequency values remaining within the deadband margin.
- When conducting the battery lifetime study through capacity firming, it was observed how a higher State of Charge (SoC) impacts calendar degradation. Additionally, when the battery is cycling, the degradation is influenced by the number of cycles, their average SoC, and their depth.
- When analyzing the battery lifetime during Frequency Containment Reserve (FCR) operation, a relationship was found between the frequency input—remaining within the deadband for 80% of the year—and calendar degradation. In this service, degradation was primarily due to calendar aging, as the battery spent most of the time idling because no power was required to correct over- or under-frequency events. A

degradation due to calendar aging of 2.4335% was observed, while cycling-related degradation was significantly lower at 0.9234%. This results is the longest battery lifetime among the analyzed services, with an estimated End of Life at 5.96 years.

- In the case of combining both services, it has been observed that by prioritizing the FCR service and fulfilling capacity firming only when the battery is capable, the resulting End of Life (EOL) lies between the two individual services, at 5.62 years. The degradation due to cycling operation when both services are combined is the highest among all cases, reaching 2.1932%, compared to 2.1186% for capacity firming alone. On the other hand, the time spent in idling mode is the lowest when services are combined, resulting in the lowest degradation due to calendar aging at 1.3625%, whereas capacity firming led to 1.7917%. The shortest battery lifetime was observed during capacity firming operation, with an EOL of 5.11 years.
- The objectives of this project have been successfully achieved. A framework has been developed for different grid services, allowing for the analysis and study of battery degradation in each service individually as well as in combined operation.

6.2 Future Work

The results in this master thesis can be extended by following the summarized below:

- Different strategies for providing FCR could be analyzed and compared. For instance, the battery could participate exclusively in up-regulation or down-regulation, or, in the case of participating in both, its state of charge (SoC) could be set at 50% and only re-establish when reach the SoC boundaries.
- In the capacity firming service, which is based on creating scheduled power steps every 15 minutes, the study could be extended by implementing different power schedule steps and comparing their impact.
- An attempt could be made to build a small-scale setup with solar panels and a battery in order to conduct this study, initially performing each service individually and eventually both services together.
- Laboratory validation of the lifetime results could be performed.

Bibliography

[1] Tze-Zhang Ang et al. "A comprehensive study of renewable energy sources: Classifications, challenges and suggestions". In: *Energy Strategy Reviews* 43 (Sept. 2022), p. 100939. ISSN: 2211-467X. DOI: 10.1016/j.esr.2022.100939. URL: https://www.sciencedirect.com/science/article/pii/S2211467X2200133X.

[2] *Successful 15-minute ISP go-live – nordicbalancingmodel*. en-US. May 2023. URL: https://nordicbalancingmodel.net/successful-15-minute-isp-go-live/.

[3] Nuno Carvalho Figueiredo, Patrícia Pereira da Silva, and Pedro A. Cerqueira. "It is windy in Denmark: Does market integration suffer?" In: *Energy*. Towards low carbon energy systems: engineering and economic perspectives 115 (Nov. 2016), pp. 1385–1399. ISSN: 0360-5442. DOI: 10.1016/j.energy.2016.05.038. URL: https://www.sciencedirect.com/science/article/pii/S036054421630648X.

[4] *outlook for ancillary services 2023-2040*. URL: https://en.energinet.dk/media/jbglyjdf/outlook-for-ancillary-services-2023-2040.pdf.

[5] *Renewable Grid (Capacity) Firming | GE Vernova*. en. URL: https://www.gevernova.com/gas-power/applications/grid-firming.

[6] *ANCILLARY SERVICES TO BE DELIVERED IN DENMARK - TENDER CONDITION*. URL: https://en.energinet.dk/media/uuzfldlp/21_10162-21-ancillary-services-to-be-delivered-in-denmark-tender-conditions-10527603_1_1.pdf.

[7] *Frequency Containment Reserves*. en-us. URL: https://www.entsoe.eu/network_codes/eb/fcr/.

[8] Monika Sandelic, Daniel-Ioan Stroe, and Florin Iov. "Battery Storage-Based Frequency Containment Reserves in Large Wind Penetrated Scenarios: A Practical Approach to Sizing". en. In: *Energies* 11.11 (Nov. 2018). Number: 11 Publisher: Multidisciplinary Digital Publishing Institute, p. 3065. ISSN: 1996-1073. DOI: 10.3390/en11113065. URL: https://www.mdpi.com/1996-1073/11/11/3065.

[9] H. Saadat. *Power systems analysis, 2nd Ed. : McGraw Hill*.

[10] *TECHNICAL REGULATION 3.3.1 – REVISION 5 REQUIREMENTS FOR ENERGY STORAGE FACILITIES*. URL: https://en.energinet.dk/media/qmspag3i/technical-regulation-331-requirements-for-energy-storage-facilities-revision-5.pdf.

[11] *Eurowind Energy Launches Five Energy Centers*. en. July 2022. URL: https://eurowindenergy.com/insights/eurowind-energy-launches-five-energy-centers.

[12] *Battery size determination for photovoltaic capacity firming using deep learning irradiance forecasts - ScienceDirect*. URL: https://www.sciencedirect.com/science/article/pii/S2352152X20318594.

[13] Raluca Nelega et al. "Prediction of Power Generation of a Photovoltaic Power Plant Based on Neural Networks". In: *IEEE Access* 11 (2023). Conference Name: IEEE Access, pp. 20713–20724. ISSN: 2169-3536. DOI: 10.1109/ACCESS.2023.3249484. URL: https://ieeexplore.ieee.org/document/10054046.

[14] *A current perspective on the accuracy of incoming solar energy forecasting - ScienceDirect*. URL: https://www.sciencedirect.com/science/article/pii/S0360128518300303.

[15] Daniel-Ioan Stroe et al. "Suggested operation of grid-connected lithium-ion battery energy storage system for primary frequency regulation: Lifetime perspective". In: *2015 IEEE Energy Conversion Congress and Exposition (ECCE)*. ISSN: 2329-3748. Sept. 2015, pp. 1105–1111. DOI: 10.1109/ECCE.2015.7309813. URL: https://ieeexplore.ieee.org/document/7309813/.

[16] Daniel-Ioan Stroe et al. "Degradation Behavior of Lithium-Ion Batteries Based on Lifetime Models and Field Measured Frequency Regulation Mission Profile". In: *IEEE Transactions on Industry Applications* 52.6 (Nov. 2016), pp. 5009–5018. ISSN: 1939-9367. DOI: 10.1109/TIA.2016.2597120. URL: https://ieeexplore.ieee.org/document/7529137.

[17] Steffen Kortmann et al. "A Two-Stage Optimization for Multi-Use Operation of BESS with Peak Shaving and FCR Applications". In: *2024 IEEE Power & Energy Society General Meeting (PESGM)*. ISSN: 1944-9933. July 2024, pp. 1–5. DOI: 10.1109/PESGM51994.2024.10689185. URL: https://ieeexplore.ieee.org/document/10689185/.

[18] *Database for wind + storage co-located projects*. URL: https://windeurope.org/about-wind/database-for-wind-and-storage-colocated-projects/.

[19] Daniel-Ioan Stroe. "Lifetime Models for Lithium Ion Batteries used in Virtual Power Plants". en. In: ().

[20] João Martins et al. "Comparative Study of Ramp-Rate Control Algorithms for PV with Energy Storage Systems". en. In: *Energies* 12.7 (Apr. 2019), p. 1342. ISSN: 1996-1073. DOI: 10.3390/en12071342. URL: https://www.mdpi.com/1996-1073/12/7/1342.

[21] W. C. S. Amorim et al. “On sizing of battery energy storage systems for PV plants power smoothing”. In: *Electric Power Systems Research* 229 (Apr. 2024), p. 110114. ISSN: 0378-7796. DOI: 10.1016/j.epsr.2024.110114. URL: https://www.sciencedirect.com/science/article/pii/S0378779624000038.

Appendix A

Appendix

A.1 FCR Additional

Firstly, the frequency data for the entire month of January has been analyzed to observe how it varies throughout the month and to determine the amount of power (in pu) that needs to be injected or absorbed. As shown below, the frequency and corresponding power for the entire month are presented.

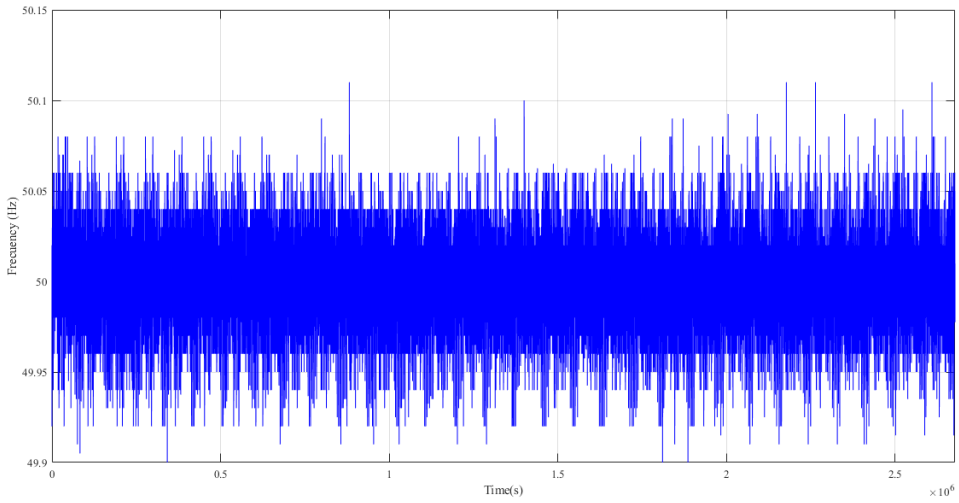

Figure A.1: Frequency each 4s during January

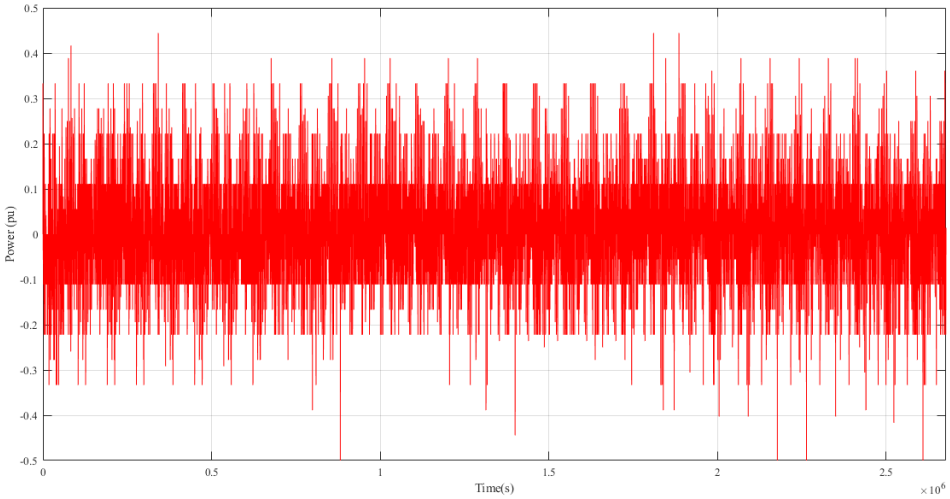

Figure A.2: Power in pu each 4s during January

A.2 Battery Model Implementation

A simplified version of the battery model is shown below in the following schematic:

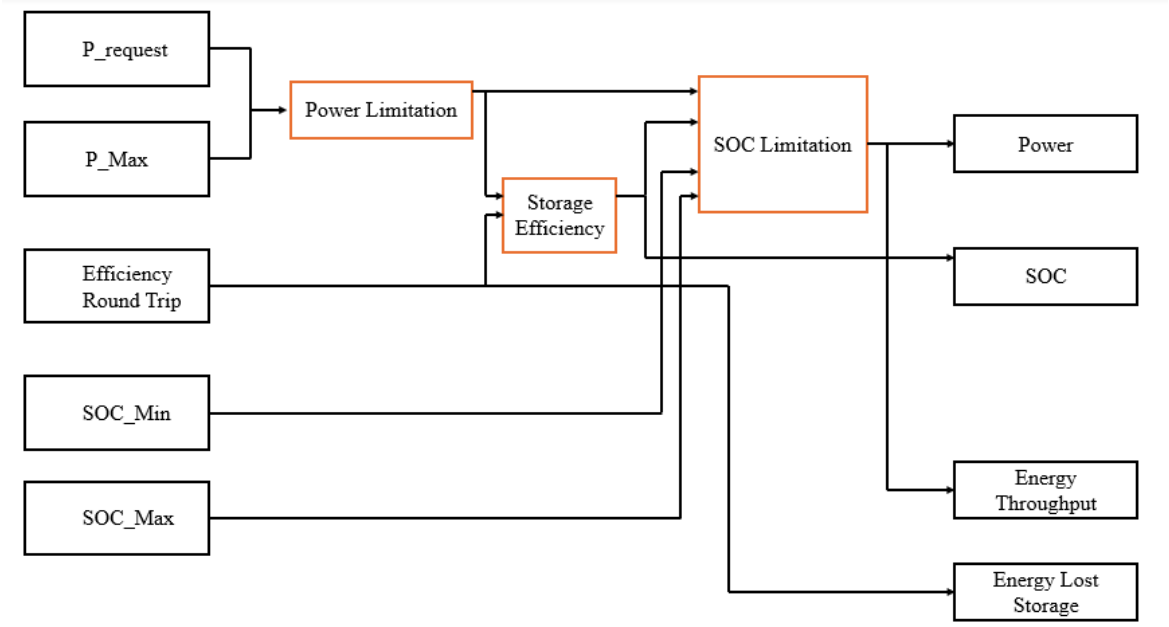

Figure A.3: Battery Model Schematic

As shown, the model is built using different blocks, and the most relevant ones are highlighted in orange, which will be explained in more detail below.

A.2.1 Power Limitation Block

The block Power Limitation is used to limit the requested power to a maximum allowable value, both in the positive and negative directions. The input to the function is the requested power P_{request} and the maximum allowed power P_{max}. The function returns the output power P_{out} according to the following condition:

$$P_{\text{out}} = \begin{cases} P_{\text{max}} & \text{if } P_{\text{request}} > P_{\text{max}} \\ -P_{\text{max}} & \text{if } P_{\text{request}} < -P_{\text{max}} \\ P_{\text{request}} & \text{otherwise} \end{cases} \tag{A.1}$$

This logic ensures that the power delivered or absorbed by the system remains within safe operational limits. If the requested power exceeds P_{max}, it is capped at P_{max}. If it is below $-P_{\text{max}}$, it is limited to $-P_{\text{max}}$. Otherwise, the requested power is accepted without modification.

A.2.2 Storage Efficiency Block

In this block the effective storage power is limited due to charging and discharging losses and this is achieved by the implementation of the following equations which describe the relationship between round-trip efficiency and the individual efficiencies during charging and discharging processes of an energy storage system. Assuming symmetrical behavior, both the charging efficiency η_{CH} and discharging efficiency η_{DCH} are defined as the square root of the round-trip efficiency η_{RT}:

$$\eta_{CH} = \sqrt{\eta_{RT}} \tag{A.2}$$

$$\eta_{DCH} = \sqrt{\eta_{RT}} \tag{A.3}$$

Using these efficiencies, the actual power required to charge the battery P_{CH} and the power delivered during discharge P_{DCH} can be calculated based on the effective energy storage power P_{ES}. During charging, the system must supply more power than what is effectively stored due to losses, which is modeled as:

$$P_{CH} = \frac{P_{ES}}{\eta_{CH}} \tag{A.4}$$

Conversely, during discharging, the system delivers less power than the stored energy due to losses, and it is given by:

$$P_{DCH} = P_{ES} \cdot \eta_{DCH} \tag{A.5}$$

These equations are essential for accurately modeling the energy flows in a battery system and assessing its efficiency under both charging and discharging operations.

A.2.3 SoC Limitation Block

The following logic ensures that the battery storage system does not exceed its operational limits in terms of state of charge (SoC). According to the control conditions, if the SoC reaches its minimum or maximum threshold, the system must not allow further charging or discharging, respectively. Therefore, the output power is set to zero in such cases. Mathematically, this is expressed as:

$$\text{Power} = P_{\text{out}} \tag{A.6}$$

$$\text{If } SOC \leq SOC_{\text{min}} \text{ and } P_{\text{out}} > 0 \Rightarrow \text{Power} = 0 \tag{A.7}$$

$$\text{If } SOC \geq SOC_{\text{max}} \text{ and } P_{\text{out}} < 0 \Rightarrow \text{Power} = 0 \tag{A.8}$$

This means that the storage system should not be able to provide the requested power if it reaches the maximum or minimum value of the SoC. In this case, the output power is forcibly limited to zero to prevent overcharging or overdischarging of the battery, thus ensuring its safe and efficient operation.

A.2.4 Verification Battery Model

To verify the battery model, the following figures are presented. In this case, there is a power request of 1.5 MW, as shown below.

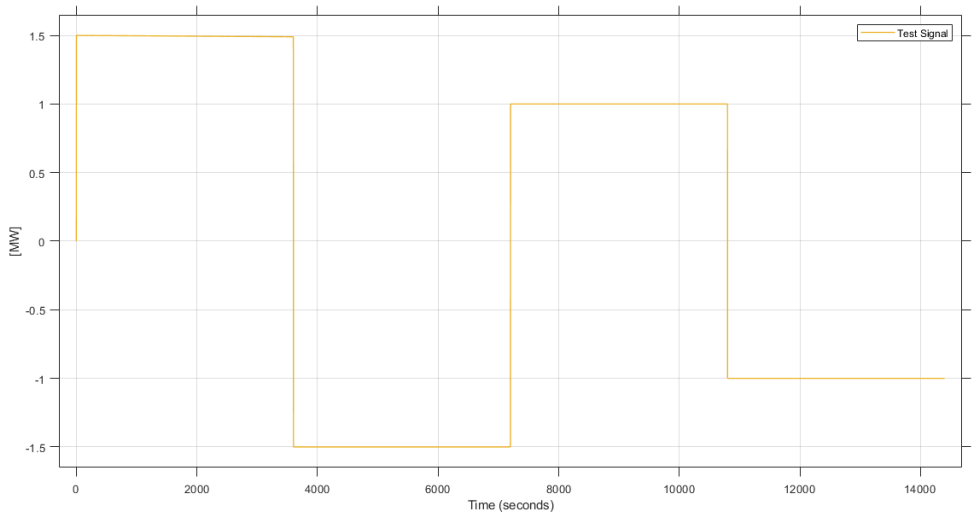

Figure A.4: Power Request Profile

Once the power request profile is shown, the SoC and the output power of the battery are presented. In this case, the initial SoC has been set to 0%, as well as the minimum SoC, while the maximum SoC is set to 100%. The battery's maximum power has been limited to 1 MW and its storage energy to 1 MWh. The round-trip efficiency has been set to 95%

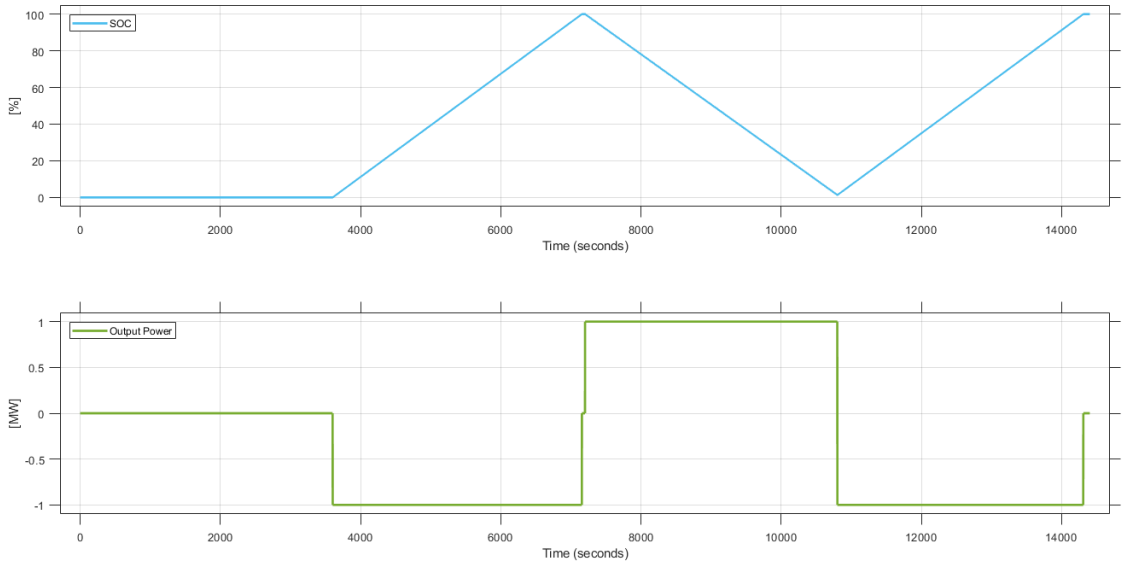

Figure A.5: SoC and Output Power Profile

As previously mentioned, the figures above show how the battery's SoC starts at 0% during the first hour, and therefore, the output power is also 0. When the battery be-

gins charging and the SoC increases, the battery power shifts to –1 MW. In this case, the negative power indicates charging. Once the battery reaches the maximum SoC limit (set to 100% in this case), there is a period during which the SoC remains at 100% and the power drops to 0 for a short time. This is followed by a discharge phase, where the SoC decreases and the power becomes +1 MW. Here, the positive power indicates discharging. This process repeats: when the SoC reaches 0% again and the battery starts charging, the power returns to –1 MW and the SoC begins to increase once more.

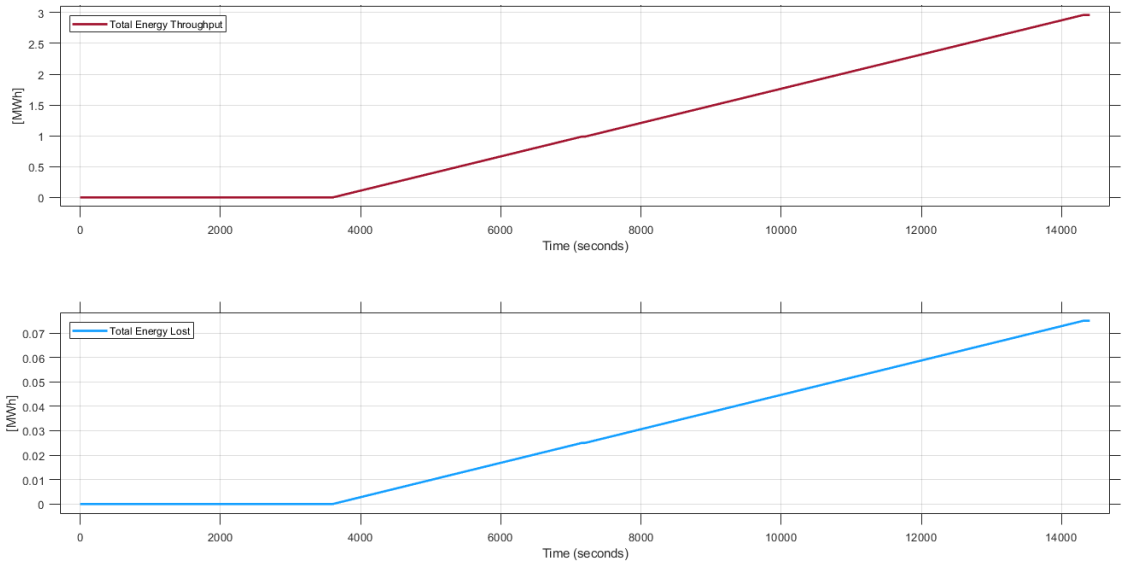

Figure A.6: Energy Throughput and Energy Lost in Storage Profile

The plots above show the cumulative energy metrics of the battery system over time. The first figure represents the Total Energy Throughput, which is the sum of all energy charged and discharged by the battery, regardless of direction. As seen, the throughput increases linearly once the battery begins to operate. Initially, during the first hour (up to around 3600 seconds), there is no energy throughput since the battery remains idle with SoC at 0%, and no power is delivered or absorbed. Once charging starts at –1 MW, the throughput begins to rise. During subsequent charging and discharging cycles, the throughput continues to increase steadily, reflecting the energy exchanges occurring during both phases.

The second plot shows the Total Energy Loss, which corresponds to the cumulative energy dissipated due to inefficiencies in the charging and discharging processes. The slope of this curve is much smaller than that of the throughput, as expected due to the round-trip efficiency (95%) of the system. Similar to the throughput plot, there is no loss recorded during the initial idle period. Once the battery starts cycling, energy losses accumulate progressively, increasing at a nearly linear rate that correlates with the throughput.

A.3 Capacity Firming Addtional

In the report, the output power of the PV plant is shown only for July to avoid a very large graph. However, below is the output power for the entire year 2023, scaled to the nominal power of the plant, which is 15 MW:

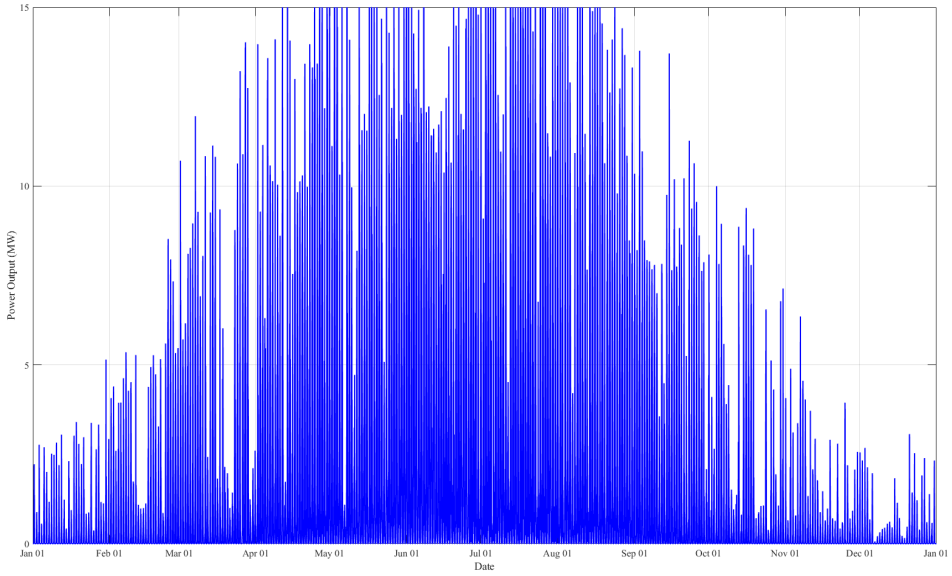

Figure A.7: Output Power PV 2023